
Scale-Dependent Radial Geometry and Metric Mismatch in Wasserstein Propagation for Reverse Diffusion

Zicheng Lyu

School of Data Science, Fudan University
lyuzicheng@gmail.com

Zengfeng Huang*

School of Data Science, Fudan University
Shanghai Innovation Institute
huangzf@fudan.edu.cn

Abstract

Existing analyses of reverse diffusion often propagate sampling error in the Euclidean geometry underlying W_2 along the entire reverse trajectory. Under weak log-concavity, however, Gaussian smoothing can create contraction first at large separations while short separations remain non-dissipative. The first usable contraction is therefore radial rather than Euclidean, creating a metric mismatch between the geometry that contracts early and the geometry in which the terminal error is measured. We formalize this mismatch through an explicit radial lower profile for the learned reverse drift. Its far-field limit gives a contraction reserve, its near-field limit gives the Euclidean load governing direct W_2 propagation, and admissible switch times are characterized by positivity of the reserve on the remaining smoothing window. We exploit this structure with a one-switch routing argument. Before the switch, reflection coupling yields contraction in a concave transport metric adapted to the radial profile. At the switch, we convert once from this metric back to W_2 under a p -moment budget, and then propagate the converted discrepancy over the remaining short window in Euclidean geometry. For discretizations of the learned reverse SDE under L^2 score-error control, a one-sided Lipschitz condition of score error, and standard well-posedness and coupling hypotheses, we obtain explicit non-asymptotic end-to-end W_2 guarantees, a scalar switch-selection objective, and a sharp structural limit on the conversion exponent within the affine-tail concave class.

1 Introduction

Score-based diffusion models are now a central framework for generative modeling, from high-fidelity image synthesis to conditional tasks such as inpainting and super-resolution [Ho et al., 2020, Song et al., 2020, Dhariwal and Nichol, 2021, Rombach et al., 2022]. At a conceptual level, sampling follows a reverse-time dynamics. The geometry of the smoothed intermediate laws governs this dynamics, score approximation perturbs it, and numerical samplers discretize it. An end-to-end theory of diffusion sampling should therefore explain, along reverse time, how geometry, initialization mismatch, score error, and discretization interact.

A growing theoretical literature has established convergence guarantees for diffusion samplers in several discrepancy measures, including KL divergence, total variation, and Wasserstein distances [Conforti et al., 2025, Lee et al., 2023, Gao et al., 2025, Gao and Zhu, 2024, Gentiloni-Silveri and Ocello, 2025]. We focus on the 2-Wasserstein distance W_2 , in which initialization mismatch, the perturbation induced by score approximation, and discretization admit a common coupling-based

*Corresponding author.

treatment. In globally regular regimes, discrepancy can often be propagated directly in W_2 over the entire reverse trajectory, without changing metric across phases [Gao et al., 2025, Gao and Zhu, 2024]. Our question is: *once global regularity is lost, what effective transport geometry becomes operative along the reverse trajectory, how does it depend on time and scale, and how should end-to-end discrepancy be propagated through it?*

We work under weak log-concavity: the target law remains globally confining but may be locally nonconvex, in the spirit of recent Ornstein–Uhlenbeck regularization analyses beyond global log-concavity [Gentiloni-Silveri and Ocello, 2025]. In this regime, Gaussian smoothing need not yield Euclidean contractivity uniformly across scales. Instead, the lower radial profile we derive can become contractive first at large separations while remaining obstructed near the origin. A standard full-horizon Euclidean propagation is therefore controlled by the short-scale obstruction, even though useful contraction is already present at larger scales. In other words, once global regularity is lost, the effective transport geometry is no longer uniformly Euclidean: it becomes scale-dependent, and this is the metric mismatch behind our analysis.

This leads to a phase-dependent routing argument. On an early window, discrepancy is propagated in a concave transport metric adapted to the radial profile. At a switch point s_0 in the forward smoothing variable—formalized later through an admissibility condition—we convert once back to W_2 , and the remaining late window is propagated in Euclidean geometry. Section 4 states the resulting one-switch routing theorem for learned reverse diffusion.

Our contributions. Our contributions are threefold.

- (i) We identify the scale-dependent transport geometry created by Gaussian smoothing under weak log-concavity. An explicit radial lower profile separates a far-field contractive regime from a near-field obstructed regime, and this one-dimensional profile characterizes admissible switch points.
- (ii) We turn this geometry into a proof mechanism. On the early window, reflection coupling reduces the separation process of two copies of the learned reverse SDE to a one-dimensional radial diffusion, from which we construct an adapted concave switch metric $W_{\varphi_{s_0}}$ (see Definition 6) that propagates initialization mismatch, score forcing, and early discretization up to the switch. We then prove a one-time conversion estimate from $W_{\varphi_{s_0}}$ back to W_2 , with exponent $\theta_p = (p-2)/(2(p-1))$ under p -moment switch control, and show that this exponent is structurally sharp within the affine-tail concave class used for the switch metric.
- (iii) We compose these ingredients into an end-to-end one-switch W_2 routing theorem together with a scalar switch-selection objective, thereby formalizing the separation from the standard direct full-horizon Euclidean route.

1.1 Technique overview

The proof is driven by a single geometric mechanism. Beyond globally regular regimes, reverse diffusion is not controlled by one uniform Euclidean dissipativity constant, but by a scale-dependent radial contractivity profile of the learned reverse drift. Under weak log-concavity, Gaussian smoothing can make this profile contractive first at large separations while the Euclidean one-sided monotonicity bound relevant for direct W_2 propagation remains non-contractive at short scales. The key issue is therefore a metric mismatch: the first usable contraction appears in a transport geometry different from the Euclidean geometry in which the terminal error is propagated.

Let p_s denote the smoothed data law at noise level s , and write $s = T - t$ for forward time along the reverse trajectory. In the score-based SDE formulation [Song et al., 2020], the ideal and learned reverse dynamics are

$$\begin{aligned} d\tilde{X}_t &= b_t(\tilde{X}_t) dt + g(T-t) d\bar{B}_t, \\ d\hat{Y}_t &= \hat{b}_t(\hat{Y}_t) dt + g(T-t) d\bar{B}_t, \end{aligned} \tag{1}$$

where b_t is the ideal reverse drift and \hat{b}_t is the learned reverse drift. For a vector field u , define its radial drift profile by

$$\kappa_u(r) := \inf_{\|x-y\|=r} -\frac{\langle u(x) - u(y), x - y \rangle}{\|x - y\|^2}, \quad r > 0.$$

Under Assumptions 1 and 3—the latter being a one-sided geometric control of the score error, rather than a global Lipschitz assumption—the radial profile dictionary in Section 3 yields

$$\kappa_{\widehat{b}_t}(r) \geq g^2(s) \left(\alpha_s - \frac{1}{r} f_{M_s}(r) - \ell(s) \right) - f(s), \quad s = T - t, \quad (2)$$

with explicit coefficients determined by smoothing and score-error control. We denote the right-hand side of (2) by $\underline{\kappa}_s(r)$.

The key point is that this single lower envelope already encodes the two geometric regimes used later:

$$\lim_{r \downarrow 0} \underline{\kappa}_s(r) = -\mathbf{b}(s), \quad \lim_{r \rightarrow \infty} \underline{\kappa}_s(r) = \mathbf{m}(s).$$

Thus $\mathbf{b}(s)$ and $\mathbf{m}(s)$ are not separate bookkeeping quantities; they are the near-field and far-field ends of the same radial lower profile. The near-field endpoint records the residual Euclidean obstruction, while the far-field endpoint records the contraction reserve created by Gaussian smoothing.

From synchronous to reflection coupling. A direct W_2 propagation uses synchronous coupling. Because the two copies are driven by the same Brownian motion, the noise cancels from the distance evolution, so a Euclidean Grönwall closure requires a global one-sided bound

$$\langle x - y, \widehat{b}_t(x) - \widehat{b}_t(y) \rangle \leq \beta(t) \|x - y\|^2, \quad x, y \in \mathbb{R}^d. \quad (3)$$

In globally regular regimes, such a closure is typically provided by a global one-sided Lipschitz control of the learned score or reverse drift [Gao et al., 2025, Gao and Zhu, 2024]. The key restriction is that (3) must hold uniformly over all radii. Hence synchronous coupling is governed by the worst value of the radial profile $r \mapsto \kappa_{\widehat{b}_t}(r)$, which in the early weakly log-concave regime comes from the near field. So the direct Euclidean route fails not because large-scale contraction is absent, but because synchronous coupling can use it only when every radius is already Euclideanly dissipative.

To exploit the full scale-dependent profile, we instead use reflection coupling [Eberle, 2016, Eberle et al., 2019]. Fix an admissible switch s_0 , and compress the early geometry into a switch-level lower envelope $\underline{\kappa}_{s_0}$, negative near the origin and positive beyond a threshold $R_{\text{sw}}(s_0)$. If Y_t and \bar{Y}_t are reflected copies of the learned reverse SDE and $r_t := \|Y_t - \bar{Y}_t\|$, then, up to coupling time, the multidimensional dynamics reduce schematically to

$$dr_t \lesssim -\underline{\kappa}_{s_0}(r_t) r_t dt + 2g(T - t) dW_t. \quad (4)$$

Unlike synchronous coupling, the radial dynamics retains a Brownian term and therefore sees the full switch-level profile rather than only its worst short-scale Euclidean value. This is exactly what makes a concave radial cost effective: applying Itô's formula to $\varphi(r_t)$ produces the second-order term $2g(T - t)^2 \varphi''(r_t)$, which can offset the near-field load.

The switch metric as an adapted radial Lyapunov gauge. The switch metric φ_{s_0} is therefore not an auxiliary softer cost chosen after the fact. It is built for the one-dimensional generator exposed by reflection coupling. Writing $\underline{g}(s_0) := \inf_{u \in [s_0, T]} g(u)$, the relevant radial operator has the schematic form

$$\mathcal{L}_{s_0} \varphi(r) = 2\underline{g}(s_0)^2 \varphi''(r) - \underline{\kappa}_{s_0}(r) r \varphi'(r).$$

We choose φ_{s_0} as an explicit concave subsolution of

$$2\underline{g}(s_0)^2 \varphi''(r) - \underline{\kappa}_{s_0}(r) r \varphi'(r) \leq -c(s_0) \varphi(r). \quad (5)$$

This is the conceptual core of the construction: the metric is adapted to the reflected radial generator before it is used as a transport cost.

The resulting switch metric is

$$\varphi_{s_0}(r) = \begin{cases} \int_0^r e^{-\lambda(s_0)u^2} du, & 0 \leq r \leq R_{\text{sw}}(s_0), \\ \varphi_{s_0}(R_{\text{sw}}(s_0)) + \mathbf{a}(s_0)(r - R_{\text{sw}}(s_0)), & r \geq R_{\text{sw}}(s_0), \end{cases} \quad (6)$$

for switch-dependent parameters $\lambda(s_0)$ and $\mathbf{a}(s_0)$. Its form matches the two ends of the profile. On $0 \leq r \leq R_{\text{sw}}(s_0)$, where $\underline{\kappa}_{s_0}$ may still be negative, the curvature term $2\underline{g}(s_0)^2 \varphi''_{s_0}$ supplied by the

reflected radial noise compensates the near-field Euclidean obstruction. On $r \geq R_{\text{sw}}(s_0)$, where the profile carries positive radial margin, no curvature is needed; the metric is continued affinely so as to retain sensitivity to large separations and hence preserve the far-field reserve.

Applying Itô's formula to $\varphi_{s_0}(r_t)$, together with (5), yields the early semigroup contraction

$$W_{\varphi_{s_0}}(\mu P_{u,v}, \nu P_{u,v}) \leq e^{-c(s_0)(v-u)} W_{\varphi_{s_0}}(\mu, \nu), \quad 0 \leq u \leq v \leq t_s := T - s_0, \quad (7)$$

where $P_{u,v}$ denotes the learned reverse semigroup. Thus the far-field reserve is converted into actual early-window transport contraction, but in an adapted concave metric rather than directly in W_2 .

This contraction compresses the entire early window into one damped switch-time quantity through the same one-step defect interface later used in the Euclidean phase. Because $\varphi_{s_0}(r) \leq r$, every one-step W_2 defect also controls the corresponding $W_{\varphi_{s_0}}$ defect.

The one-time return to W_2 and what it costs. The switch should not be read as the time at which the geometry suddenly becomes Euclidean. Its role is different: it is the point at which an already damped discrepancy is returned once to the Euclidean geometry in which the final error is measured. This return is possible because the switch metric has an affine tail,

$$\varphi_{s_0}(r) \geq \alpha(s_0) r, \quad r \geq 0,$$

so $W_{\varphi_{s_0}}$ controls a truncated linear distance. Combined with a p -moment budget at switch time, this yields the interpolation

$$W_2^2 \lesssim \frac{\rho^2}{\varphi_{s_0}(\rho)} \Delta_{\varphi}^{\text{sw}}(s_0) + \frac{\overline{\mathcal{M}}_p^{\text{sw}}(s_0)}{\rho^{p-2}},$$

and optimizing in ρ gives

$$W_2(\text{Law}(Z_{t_s}), \text{Law}(\tilde{X}_{t_s})) \lesssim C_p^{\text{sw}}(s_0) (\Delta_{\varphi}^{\text{sw}}(s_0))^{\theta_p}, \quad \theta_p = \frac{p-2}{2(p-1)}.$$

It is the quantitative price of recovering quadratic Euclidean transport from an early metric that is deliberately softer than W_2 .

The conversion is also where the central tradeoff becomes visible. A more concave early metric is better at absorbing the near-field obstruction under the reflected radial dynamics, but within the affine-tail concave class this comes with weaker quadratic sensitivity at large distances and hence a more expensive return to W_2 . The sharpness result shows that this loss is structural rather than a proof artifact: the same non-Euclidean softness that makes early damping possible also prevents a free recovery of Euclidean quadratic transport.

Late-window Euclidean propagation and optimal switching. After the switch, what remains is to propagate the converted discrepancy over the final short window in the target metric W_2 , for which synchronous coupling is again the natural tool. This yields

$$W_2(\text{Law}(Z_{t_N}), p_0) \lesssim \Delta_{\text{late}}(s_0) + e^{\Gamma(s_0)} C_p^{\text{sw}}(s_0) (\Delta_{\varphi}^{\text{sw}}(s_0))^{\theta_p}.$$

Admissibility and optimization therefore play different roles. Admissibility is a geometric existence statement: it guarantees that a genuinely non-Euclidean contractive regime is available on the early window. Optimal switching is a routing statement: it decides when the already compressed discrepancy should be re-exposed to W_2 , balancing how much early damping remains available, how expensive the one-time conversion is, and how much late Euclidean load is left.

Organization. Section 2 positions the paper relative to existing diffusion-model convergence theory. Section 3 introduces the reverse-diffusion setting, the structural assumptions, and the radial geometry of the learned drift. Section 4 states the main theorem and explains its meaning. Section 5 returns to the geometric message and the open directions.

2 Related Work

Our work lies at the intersection of Wasserstein convergence theory for score-based generative models, analyses of reverse-time geometry beyond global log-concavity, and reflection-coupling contraction methods for nonconvex diffusions.

W_2 theory under regular and changing geometry. A broad theoretical literature studies diffusion sampling under minimal assumptions or in KL/path-space metrics [Chen et al., 2022, 2023a, Lee et al., 2023]. Within W_2 , globally regular regimes admit direct full-horizon Euclidean propagation for reverse SDEs and PFODEs [Gao et al., 2025, Gao and Zhu, 2024]. More recent W_2 analyses move beyond global log-concavity, including Gaussian-tail, semiconvex, and weakly log-concave settings [Wang and Wang, 2024, Bruno and Sabanis, 2025, Gentiloni-Silveri and Ocello, 2025]. The three closest comparisons emphasize different aspects of time-varying geometry. Gentiloni-Silveri and Ocello [2025] shows that weak log-concavity can produce alternating contractive and non-contractive phases along reverse time; Bruno and Sabanis [2025] studies semiconvex settings with time-dependent Euclidean W_2 control; and Wang and Wang [2024] obtains Euclidean/PDE-based bounds under Gaussian-tail assumptions. Our result is complementary to these works. The additional point we emphasize is not only *when* contractivity appears, but also *in which metric* it first becomes exploitable: a reverse trajectory may already contract in a softer radial transport geometry even while direct Euclidean closure is still blocked by the near field. This is the metric-mismatch principle behind the one-switch route.

Reflection coupling and concave transport metrics. Methodologically, we build on the reflection-coupling line for diffusions with nonconvex geometry, from the classical multidimensional diffusion constructions of Lindvall and Rogers [1986], Chen and Li [1989] to the concave-cost contraction framework of Eberle [2016], Eberle et al. [2019]. We use the Gaussian-smoothed radial profile of the learned reverse drift to determine an early-window concave transport metric, propagate score and discretization errors on that window, and then perform a single return to W_2 . Our distinctive contribution is therefore the reverse-diffusion interface and one-switch routing theorem, not reflection coupling in isolation.

Sampler interfaces. A complementary line develops convergence analyses for deterministic, stochastic, and higher-order samplers [Chen et al., 2023b, Li et al., 2024, Beyler and Bach, 2025, Yu and Yu, 2025, Pfarr et al., 2026], as well as sharper complexity or stability/forgetting guarantees [Benton et al., 2023, Chen et al., 2026, Strasman et al., 2026]. Here the relation is especially direct. Results such as Beyler and Bach [2025] and Pfarr et al. [2026] provide local or global W_2 discretization estimates for deterministic, stochastic, and higher-order schemes. In our theorem, those estimates populate the one-step defect interface ξ_k : once ξ_k is available, the routing bound determines how much of that sampler error is damped on the early radial window and how much is exposed to the late Euclidean window. Thus better orders or smaller constants from EM, Heun, PF-ODE, or higher-order analyses can be imported directly without changing the geometric part of the proof. Accordingly, our result is not broader sampler coverage or sharper complexity guarantees, but a propagation principle that separates the metric in which contraction first appears from the metric in which the final error is measured.

3 Reverse-diffusion interface and time-dependent radial geometry

This section sets up the reverse diffusion and isolates the scale-dependent geometry used in the theorem. Under weak log-concavity, Gaussian smoothing can stabilize large separations before short scales satisfy a Euclidean one-sided dissipativity bound. We formalize this through a radial profile of the learned reverse drift and the quantities extracted from its two ends.

Notation. We use the Euclidean inner product and norm throughout, write $\mathcal{P}_p(\mathbb{R}^d)$ for laws with finite p -th moment, and for probability measures μ, ν on \mathbb{R}^d let $\Pi(\mu, \nu)$ denote the set of couplings of μ and ν , i.e. the Borel probability measures on $\mathbb{R}^d \times \mathbb{R}^d$ with marginals μ and ν . We denote the 2-Wasserstein distance by W_2 , and parametrize reverse time by $t := T - s$.

3.1 Forward smoothing and reverse interface

Let $p_0(dx) \propto e^{-V_0(x)} dx$, where $V_0 \in C^1(\mathbb{R}^d)$ and $\int_{\mathbb{R}^d} e^{-V_0(x)} dx < \infty$. Given Borel measurable $f, g : [0, T] \rightarrow \mathbb{R}_{\geq 0}$ with $\int_0^T f(u) du < \infty$, $\int_0^T g^2(u) du < \infty$, and $g(s) > 0$ for every $s > 0$, consider the forward diffusion

$$dX_s = -f(s)X_s ds + g(s) dB_s, \quad X_0 \sim p_0. \quad (8)$$

Writing

$$a(s) := \exp\left(-\int_0^s f(u) \, du\right), \quad \sigma^2(s) := \int_0^s \left(\frac{a(s)}{a(u)} g(u)\right)^2 \, du, \quad (9)$$

its marginal law is

$$p_s = (S_{a(s)} p_0) * \mathcal{N}(0, \sigma^2(s) I_d), \quad s > 0, \quad (10)$$

where $S_a \mu$ is the pushforward of μ under $x \mapsto ax$. Thus forward time acts by a deterministic linear shrinkage followed by Gaussian convolution.

The corresponding reverse drifts are

$$b_t(x) = f(T-t)x + g^2(T-t) \nabla \log p_{T-t}(x), \quad \widehat{b}_t(x) = f(T-t)x + g^2(T-t) s_\theta(x, T-t), \quad (11)$$

and the ideal and learned reverse SDEs are Anderson [1982], Haussmann and Pardoux [1986]

$$d\widetilde{X}_t = b_t(\widetilde{X}_t) \, dt + g(T-t) \, d\overline{B}_t, \quad \widetilde{X}_0 \sim p_T, \quad (12)$$

$$d\widehat{Y}_t = \widehat{b}_t(\widehat{Y}_t) \, dt + g(T-t) \, d\overline{B}_t, \quad \widehat{Y}_0 \sim \widehat{p}_T. \quad (13)$$

With

$$e_s(x) := s_\theta(x, s) - \nabla \log p_s(x), \quad s \in (0, T],$$

the drift mismatch is exactly

$$\widehat{b}_t - b_t = g^2(T-t) e_{T-t}. \quad (14)$$

Whenever the learned reverse SDE (13) is well posed on an interval $[u, v] \subseteq [0, T]$, we write $P_{u,v}$ for its transition kernel. Background facts on time reversal, regularity, and well posedness are collected in Appendix A.

Definition 1 (Strong well posedness on an interval). We say that the learned reverse SDE is strongly well posed on an interval $[u, v] \subseteq [0, T]$ if for every \mathcal{F}_u -measurable initial condition ξ with $\text{Law}(\xi) \in \mathcal{P}_1(\mathbb{R}^d)$, there exists a pathwise unique strong solution on $[u, v]$.

3.2 Structural assumptions

Assumption 1 (Weak log-concavity Gentiloni-Silveri and Ocello [2025]). Let $\alpha, M > 0$, and define $f_M(r) := 2\sqrt{M} \tanh\left(\frac{1}{2}\sqrt{M}r\right)$. Assume that for every $r > 0$,

$$\inf_{\|x-y\|=r} \frac{\langle \nabla V_0(x) - \nabla V_0(y), x-y \rangle}{\|x-y\|^2} \geq \alpha - \frac{1}{r} f_M(r).$$

Assumption 2 (Average score forcing in $L^2(p_s)$). Assume there exists a measurable function $\varepsilon : (0, T] \rightarrow [0, \infty)$ such that

$$\mathbb{E}_{X \sim p_s} \|e_s(X)\|^2 \leq \varepsilon^2(s), \quad s \in (0, T],$$

and $s \mapsto g^2(s)\varepsilon(s)$ is integrable on $(0, T]$.

Assumption 3 (One-sided Lipschitz of the score error). Assume Assumption 2 holds, and that there exists a measurable function $\ell : (0, T] \rightarrow \mathbb{R}$ such that

$$\langle e_s(x) - e_s(y), x-y \rangle \leq \ell(s) \|x-y\|^2, \quad x, y \in \mathbb{R}^d.$$

Remark 1 (On the score-error assumptions). Assumption 2 controls the size of the forcing term, whereas Assumption 3 is the theorem-level geometric condition on the score error that enters pairwise distance evolution through the one-sided Lipschitz $\ell(s)$. The latter is not vacuous and should not be read as a black-box global regularity requirement: Appendix G records standard sufficient conditions implying it.

3.3 A radial profile dictionary and admissible switches

What drives the proof is not a single Euclidean one-sided Lipschitz constant, but a family of radial lower envelopes $r \mapsto \underline{\kappa}_s(r)$, one for each noise level s . The key point is that one and the same formula already contains the near-field Euclidean obstruction and the far-field contraction reserve created by smoothing.

Definition 2 (Drift profile). For a Borel vector field $u : \mathbb{R}^d \rightarrow \mathbb{R}^d$, define its radial drift profile by

$$\kappa_u(r) := \inf_{\substack{x \neq y \\ \|x-y\|=r}} -\frac{\langle u(x) - u(y), x - y \rangle}{\|x - y\|^2}, \quad r > 0. \quad (15)$$

Positive $\kappa_u(r)$ means contraction at separation r , while negative $\kappa_u(r)$ means expansion.

Gaussian smoothing transfers the weak-log-concavity parameters (α, M) of p_0 into the time-dependent quantities

$$\alpha_s := \frac{\alpha}{a^2(s) + \alpha \sigma^2(s)}, \quad M_s := \frac{M a^2(s)}{(a^2(s) + \alpha \sigma^2(s))^2}, \quad s \in [0, T]. \quad (16)$$

Here α_s is the effective large-scale convexity of p_s , whereas M_s measures the residual short-scale nonconvexity after smoothing.

Definition 3. For $s \in (0, T]$, define

$$\mathbf{m}(s) := g^2(s)(\alpha_s - \ell(s)) - f(s), \quad \mathbf{b}(s) := f(s) + g^2(s)(M_s + \ell(s) - \alpha_s), \quad (17)$$

and the radial lower envelope

$$\underline{\kappa}_s(r) := g^2(s)\left(\alpha_s - \frac{1}{r}f_{M_s}(r) - \ell(s)\right) - f(s), \quad r > 0. \quad (18)$$

For each fixed s , the same lower envelope can be rewritten as

$$\underline{\kappa}_s(r) = \mathbf{m}(s) - g^2(s)\frac{1}{r}f_{M_s}(r) = -\mathbf{b}(s) + g^2(s)\left(M_s - \frac{1}{r}f_{M_s}(r)\right), \quad r > 0. \quad (19)$$

This identity makes the geometry explicit: $\mathbf{m}(s)$ is the far-field reserve, while the radius-dependent penalty $g^2(s)f_{M_s}(r)/r$ is largest near the origin and vanishes at infinity. Hence the reserve is converted into the Euclidean load $-\mathbf{b}(s)$ at short scales and reappears at large scales.

Lemma 1. Under Assumptions 1 and 3, for $t \in [0, T]$ and $s := T - t$, the following hold:

(i) Profile transfer. For every $r > 0$,

$$\kappa_{\widehat{b}_t}(r) \geq \underline{\kappa}_s(r). \quad (20)$$

(ii) Endpoint structure. For each fixed $s \in (0, T]$, the map $r \mapsto \underline{\kappa}_s(r)$ is nondecreasing on $(0, \infty)$, with

$$\lim_{r \downarrow 0} \underline{\kappa}_s(r) = -\mathbf{b}(s), \quad \lim_{r \rightarrow \infty} \underline{\kappa}_s(r) = \mathbf{m}(s). \quad (21)$$

If $\mathbf{m}(s) > 0$, then

$$R(s) := \inf\{r > 0 : \underline{\kappa}_s(r) \geq 0\} < \infty, \quad (22)$$

and $\underline{\kappa}_s(r) \geq 0$ for all $r \geq R(s)$.

(iii) Companion Euclidean load. For every $x, y \in \mathbb{R}^d$,

$$\langle x - y, \widehat{b}_t(x) - \widehat{b}_t(y) \rangle \leq \mathbf{b}(s)\|x - y\|^2. \quad (23)$$

The left panel is pointwise in s , whereas the right panel records the stronger uniform-in-time requirement that will define admissible switches.

Definition 4 (Admissible switches). For $s \in [0, T]$ and $s_0 \in (0, T]$, define

$$\Gamma(s) := \int_0^s \mathbf{b}(u) \, du, \quad \underline{m}(s_0) := \inf_{u \in [s_0, T]} \mathbf{m}(u),$$

whenever the integral defining $\Gamma(s)$ is finite. We call s_0 an *admissible switch* if $\underline{m}(s_0) > 0$, and write

$$\mathcal{S}_{\text{adm}} := \{s_0 \in (0, T] : \underline{m}(s_0) > 0\}.$$

For the standard VP schedule, admissibility can be certified by an explicit scalar threshold; see Proposition 8. While M does not affect bare admissibility, it still enters the early metric through M_s .

The running infimum $\underline{m}(s_0)$ appears because the early phase needs a positive far-field tail on the whole interval $[s_0, T]$, not only at one instantaneous noise level. Admissibility therefore guarantees the existence of a genuinely non-Euclidean contractive regime on the early window, but it does not require the near-field Euclidean obstruction to have vanished there. That remaining short-scale obstruction is exactly why an adapted switch metric is still needed before returning to W_2 .

For each admissible switch s_0 , the appendices construct an associated switch metric $W_{\varphi_{s_0}}$, an early damping rate $c(s_0)$, and an affine-tail slope $\alpha(s_0)$.

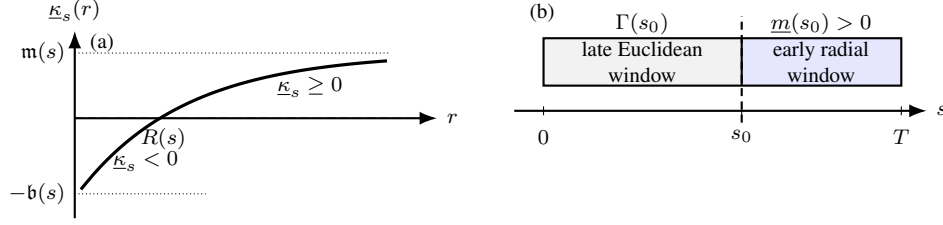


Figure 1: (a) Pointwise radial lower profile at a fixed noise level s : $\kappa_s(r)$ starts at $-b(s)$, crosses zero at $R(s)$, and approaches $m(s)$. (b) Window-level quantities used by the theorem: $\underline{m}(s_0) = \inf_{u \in [s_0, T]} m(u)$ and $\Gamma(s_0) = \int_{s_0}^{s_0} b(u) du$. Thus s_0 is admissible exactly when $\underline{m}(s_0) > 0$. The right panel is schematic and does not represent the evolution of $R(s)$.

4 A routing theorem from radial metric mismatch

Section 3 extracted the geometric inputs carried by the theorem: the radial lower envelopes κ_s , the admissible switch set \mathcal{S}_{adm} , and the late-window Euclidean load Γ . We now state the one-switch routing theorem.

For an admissible switch s_0 , write

$$\underline{g}(s_0) := \inf_{u \in [s_0, T]} g(u), \quad \bar{b}(s_0) := \sup_{u \in [s_0, T]} b(u), \quad \bar{G}(s_0) := \sup_{u \in [s_0, T]} g^2(u) \sqrt{M_u}.$$

For any increasing concave function $\varphi : [0, \infty) \rightarrow [0, \infty)$ with $\varphi(0) = 0$, define

$$W_\varphi(\mu, \nu) := \inf_{\pi \in \Pi(\mu, \nu)} \int_{\mathbb{R}^d \times \mathbb{R}^d} \varphi(\|x - y\|) \pi(dx, dy).$$

4.1 Main theorem

Work under Assumptions 1, 2 and 3. Let $0 = t_0 < \dots < t_N = T$ be a numerical grid, let $(Z_{t_k})_{k=0}^N$ be a Markovian discretization of the learned reverse SDE, and write $P_k := P_{t_k, t_{k+1}}$ and Ψ_k for the exact and numerical one-step kernels. Assume that the ideal reverse SDE (12) admits a global solution $(\tilde{X}_t)_{0 \leq t \leq T}$ on $[0, T]$ such that

$$\text{Law}(\tilde{X}_t) = p_{T-t}, \quad t \in [0, T].$$

and that the one-step defects satisfy

$$W_2(P_k(x, \cdot), \Psi_k(x, \cdot)) \leq \xi_k(x), \quad x \in \mathbb{R}^d, \quad k = 0, \dots, N-1, \quad (24)$$

for Borel measurable functions $\xi_k : \mathbb{R}^d \rightarrow [0, \infty)$.

Theorem 1. Fix $p > 2$ and assume $\hat{p}_T \in \mathcal{P}_p(\mathbb{R}^d)$. Let $s_0 \in \mathcal{S}_{\text{adm}}$ be a grid-aligned admissible switch, set $t_s := T - s_0 = t_K$, and let φ_{s_0} , $c(s_0)$, and $\mathfrak{a}(s_0)$ denote the associated switch metric, early damping rate, and affine-tail slope. Assume that the learned reverse SDE is strongly well posed on $[0, T]$, and that for every $[u, v] \subseteq [0, t_s]$ and every initial coupling $\pi \in \Pi(\mu, \nu)$ with $\mu, \nu \in \mathcal{P}_1(\mathbb{R}^d)$, there exists a coalescing reflection coupling on $[u, v]$ whose initial law is π , and that $\underline{g}(s_0) > 0$, $\bar{b}(s_0) < \infty$, $\bar{G}(s_0) < \infty$, $\Gamma(s_0) < \infty$. Let $\overline{\mathcal{M}}_p^{\text{sw}}(s_0) < \infty$ and satisfy

$$\overline{\mathcal{M}}_p^{\text{sw}}(s_0) \geq \mathbb{E} \|Z_{t_s}\|^p + \mathbb{E}_{X \sim p_{s_0}} \|X\|^p. \quad (25)$$

Then

$$W_2(\text{Law}(Z_{t_N}), p_0) \leq \Delta_{\text{late}}(s_0) + e^{\Gamma(s_0)} C_p^{\text{sw}}(s_0) \left(\overline{\Delta}_\varphi^{\text{sw}}(s_0) \right)^{\theta_p}, \quad (26)$$

where

$$\theta_p := \frac{p-2}{2(p-1)}, \quad C_p^{\text{sw}}(s_0) := \sqrt{2(p-1)} (p-2)^{-\theta_p} \mathfrak{a}(s_0)^{-\theta_p} \left(\overline{\mathcal{M}}_p^{\text{sw}}(s_0) \right)^{\frac{1}{2(p-1)}},$$

and

$$\begin{aligned} \overline{\Delta}_\varphi^{\text{sw}}(s_0) &:= e^{-c(s_0)t_s} W_{\varphi_{s_0}}(\widehat{p}_T, p_T) + \sum_{k=0}^{K-1} e^{-c(s_0)(t_s-t_{k+1})} \left(\mathbb{E}[\xi_k(Z_{t_k})^2] \right)^{1/2} \\ &\quad + \int_{s_0}^T e^{-c(s_0)(s-s_0)} g^2(s) \varepsilon(s) \, ds, \quad (27) \\ \Delta_{\text{late}}(s_0) &:= \sum_{k=K}^{N-1} e^{\Gamma(T-t_{k+1})} \left(\mathbb{E} \xi_k(Z_{t_k})^2 \right)^{1/2} + \int_0^{s_0} e^{\Gamma(s)} g^2(s) \varepsilon(s) \, ds. \end{aligned}$$

Theorem 1 is a routing statement. On $[0, t_s]$, the usable contraction is carried by the radial metric $W_{\varphi_{s_0}}$, not by Euclidean W_2 . At t_s , the damped switch-time discrepancy is converted once back to W_2 , which is exactly where the exponent $\theta_p = (p-2)/(2(p-1))$ enters; on $[t_s, T]$, the remaining error is then propagated in Euclidean geometry.

This perspective also clarifies the role of the exponent $\theta_p = (p-2)/(2(p-1))$. It enters only through the one-time conversion from $W_{\varphi_{s_0}}$ back to W_2 ; it plays no role in the early reflection-coupling contraction and no role in the late Euclidean propagation. Writing

$$\Delta_\varphi^{\text{sw}}(s_0) := W_{\varphi_{s_0}}(\text{Law}(Z_{t_s}), p_{s_0})$$

for the actual switch-time discrepancy, the theorem controls this quantity through the explicit envelope provided by Lemma 14 together with the admissible switch-time moment budget from Proposition 2. The appendices make this interface concrete. In particular, Section D, especially Section D.2, shows that within the affine-tail concave class considered here and under only a p -moment budget at switch time, the exponent θ_p is structurally sharp: it is exactly the price of recovering quadratic Euclidean transport from a deliberately softer early metric. Moreover, Section E packages the right-hand side of (26) into the scalar objective $\mathcal{B}_p(s_0)$ and proves the discrete optimal-switch corollary Corollary 2; Section F.2 compares this route with the direct full-horizon Euclidean argument; and Section G records concrete sufficient conditions verifying the theorem-level hypotheses, including standard Lipschitz and linear-growth conditions for the reflection-coupling input, conservative proxy switches, and the explicit variance-preserving example in Proposition 8.

5 Conclusion

This paper shows that, beyond globally regular regimes, reverse diffusion should not be summarized by a single Euclidean dissipativity constant. Under weak log-concavity, Gaussian smoothing can generate contraction first in the radial far field while short scales remain obstructed in the Euclidean metric underlying W_2 . The far-field reserve and the near-field obstruction are thus not competing effects, but two manifestations of the same radial geometry. The main difficulty is therefore geometric rather than purely dynamical: contraction may already be present before it becomes visible in the Euclidean metric of the final objective.

Our contribution is to formulate this mismatch as a routing principle. The analysis should proceed in the first geometry that truly contracts, extract its gain on the early window, and return to W_2 only when that return becomes favorable. In our setting, the relevant early geometry is radial rather than Euclidean; reflection coupling is therefore not the source of this geometry, but the natural device for accessing its one-dimensional distance dynamics. The induced concave metric records the resulting early contraction, and a single switch transports the damped discrepancy back to the Euclidean metric of the terminal objective. The exponent θ_p is then the structural price of this return: within the affine-tail concave class and under a p -moment budget, it is sharp.

Our analysis is restricted to weakly log-concave targets and to theorem-level hypotheses. The present theory is also intrinsically one-switch: it does not yet cover multi-switch, strongly anisotropic, or more intricate multiscale geometries, nor does it aim at sampler-specific optimal complexity bounds. Extending the framework beyond one switch, beyond affine-tail concave switch metrics, or to settings with weaker regularity remains open.

References

- Brian DO Anderson. Reverse-time diffusion equation models. *Stochastic Processes and their Applications*, 12(3):313–326, 1982.
- Joe Benton, Valentin De Bortoli, Arnaud Doucet, and George Deligiannidis. Nearly d -linear convergence bounds for diffusion models via stochastic localization. *arXiv preprint arXiv:2308.03686*, 2023.
- Eliot Beyler and Francis Bach. Convergence of deterministic and stochastic diffusion-model samplers: A simple analysis in wasserstein distance. *arXiv preprint arXiv:2508.03210*, 2025.
- Stefano Bruno and Sotirios Sabanis. Wasserstein convergence of score-based generative models under semiconvexity and discontinuous gradients. *arXiv preprint arXiv:2505.03432*, 2025.
- Fan Chen, Sinho Chewi, Constantinos Daskalakis, and Alexander Rakhlin. High-accuracy sampling for diffusion models and log-concave distributions. *arXiv preprint arXiv:2602.01338*, 2026.
- Hongrui Chen, Holden Lee, and Jianfeng Lu. Improved analysis of score-based generative modeling: User-friendly bounds under minimal smoothness assumptions. In *International Conference on Machine Learning*, pages 4735–4763. PMLR, 2023a.
- Mu-Fa Chen and Shao-Fu Li. Coupling methods for multidimensional diffusion processes. *The Annals of Probability*, pages 151–177, 1989.
- Sitan Chen, Sinho Chewi, Jerry Li, Yuanzhi Li, Adil Salim, and Anru R Zhang. Sampling is as easy as learning the score: theory for diffusion models with minimal data assumptions. *arXiv preprint arXiv:2209.11215*, 2022.
- Sitan Chen, Sinho Chewi, Holden Lee, Yuanzhi Li, Jianfeng Lu, and Adil Salim. The probability flow ode is provably fast. *Advances in Neural Information Processing Systems*, 36:68552–68575, 2023b.
- Giovanni Conforti. Weak semiconvexity estimates for schrödinger potentials and logarithmic sobolev inequality for schrödinger bridges. *Probability Theory and Related Fields*, 189(3):1045–1071, 2024.
- Giovanni Conforti, Alain Durmus, and Marta Gentiloni Silveri. Kl convergence guarantees for score diffusion models under minimal data assumptions. *SIAM Journal on Mathematics of Data Science*, 7(1):86–109, 2025.
- Prafulla Dhariwal and Alexander Nichol. Diffusion models beat gans on image synthesis. *Advances in neural information processing systems*, 34:8780–8794, 2021.
- Andreas Eberle. Reflection couplings and contraction rates for diffusions. *Probability theory and related fields*, 166(3):851–886, 2016.
- Andreas Eberle, Arnaud Guillin, and Raphael Zimmer. Couplings and quantitative contraction rates for langevin dynamics. 2019.
- Xuefeng Gao and Lingjiong Zhu. Convergence analysis for general probability flow odes of diffusion models in wasserstein distances. *arXiv preprint arXiv:2401.17958*, 2024.
- Xuefeng Gao, Hoang M Nguyen, and Lingjiong Zhu. Wasserstein convergence guarantees for a general class of score-based generative models. *Journal of machine learning research*, 26(43): 1–54, 2025.
- Marta Gentiloni-Silveri and Antonio Ocello. Beyond log-concavity and score regularity: Improved convergence bounds for score-based generative models in w_2 -distance. *arXiv preprint arXiv:2501.02298*, 2025.
- Ulrich G Haussmann and Etienne Pardoux. Time reversal of diffusions. *The Annals of Probability*, pages 1188–1205, 1986.

- Jonathan Ho, Ajay Jain, and Pieter Abbeel. Denoising diffusion probabilistic models. *Advances in neural information processing systems*, 33:6840–6851, 2020.
- Holden Lee, Jianfeng Lu, and Yixin Tan. Convergence of score-based generative modeling for general data distributions. In *International Conference on Algorithmic Learning Theory*, pages 946–985. PMLR, 2023.
- Runjia Li, Qiwei Di, and Quanquan Gu. Unified convergence analysis for score-based diffusion models with deterministic samplers. *arXiv preprint arXiv:2410.14237*, 2024.
- Torgny Lindvall and L Cris G Rogers. Coupling of multidimensional diffusions by reflection. *The Annals of Probability*, pages 860–872, 1986.
- Emanuel Pfarr, Radu Timofte, and Frank Werner. Analyzing the error of generative diffusion models: From euler-maruyama to higher-order schemes. *arXiv preprint arXiv:2601.18425*, 2026.
- Robin Rombach, Andreas Blattmann, Dominik Lorenz, Patrick Esser, and Björn Ommer. High-resolution image synthesis with latent diffusion models. In *Proceedings of the IEEE/CVF conference on computer vision and pattern recognition*, pages 10684–10695, 2022.
- Yang Song, Jascha Sohl-Dickstein, Diederik P Kingma, Abhishek Kumar, Stefano Ermon, and Ben Poole. Score-based generative modeling through stochastic differential equations. *arXiv preprint arXiv:2011.13456*, 2020.
- Stanislas Strasman, Gabriel Cardoso, Sylvain Le Corff, Vincent Lemaire, and Antonio Ocello. On forgetting and stability of score-based generative models. *arXiv preprint arXiv:2601.21868*, 2026.
- Xixian Wang and Zhongjian Wang. Wasserstein bounds for generative diffusion models with gaussian tail targets. *arXiv preprint arXiv:2412.11251*, 2024.
- Yifeng Yu and Lu Yu. Advancing wasserstein convergence analysis of score-based models: Insights from discretization and second-order acceleration. *arXiv preprint arXiv:2502.04849*, 2025.
- Xicheng Zhang. Stochastic monge–kantorovich problem and its duality. *Stochastics An International Journal of Probability and Stochastic Processes*, 85(1):71–84, 2013.

Appendix roadmap. The appendix is organized as follows. Section A develops the reverse-diffusion background and the Gaussian-smoothing profile calculus that produces the quantities α_s , M_s , $\mathfrak{m}(s)$, and $\mathfrak{b}(s)$. Section B transfers that profile to the learned drift and characterizes admissible switches. Section C proves early-window contraction in the switch metric via reflection coupling and packages the pre-switch initialization, discretization, and score-forcing contributions. Section D proves the one-time conversion from $W_{\varphi_{s_0}}$ back to W_2 , including the explicit switch-time moment budget and the sharpness of the exponent θ_p . Section E propagates the converted discrepancy through the late Euclidean window, while Section F combines all pieces into the main theorem, derives the optimized-switch corollary, and compares the one-switch route with the direct full-horizon Euclidean argument. Finally, Section G records operational supplements: proxy switches, verifiable sufficient conditions for the reflection-coupling input, and the variance-preserving worked example.

A Reverse-diffusion background and Gaussian smoothing

This section isolates the only forward-time regularization input used later. All subsequent quantities α_s , M_s , $\mathfrak{m}(s)$, and $\mathfrak{b}(s)$ ultimately come from the representation

$$p_s = (S_{a(s)}p_0) * \gamma_{\sigma^2(s)}.$$

For the theorem, it is not enough to know qualitatively that Gaussian smoothing improves geometry. We need the exact way in which smoothing acts on the weak profile

$$\kappa_{V_0}(r) \geq \alpha - \frac{1}{r} f_M(r).$$

There are three operations behind the formulas proved below: deterministic scaling by $a(s)$, which weakens both curvature and defect by the factor $a(s)^{-2}$; Gaussian convolution, which preserves the weak semiconvex defect once the available quadratic part has been peeled off; and a quadratic tilt, which returns part of that peeled-off curvature in explicit form. The outcome is the pair (α_s, M_s) : α_s records the large-scale convexity that survives smoothing, while M_s records the residual short-scale defect that smoothing has not yet erased. Nothing in this section depends on the later metric switch. Its outputs are the explicit profile bound for $V_s := -\log p_s$ and the moment bounds used at switch time.

Throughout, we use the drift profile from Definition 2. When $h \in C^1(\mathbb{R}^d)$ is a potential, we write

$$\kappa_h(r) := \kappa_{-\nabla h}(r) = \inf_{\substack{x \neq y \\ \|x-y\|=r}} \frac{\langle \nabla h(x) - \nabla h(y), x - y \rangle}{\|x - y\|^2}, \quad r > 0.$$

Thus κ_h is simply the profile of the gradient drift $-\nabla h$.

A.1 Forward smoothing and basic regularity

Lemma 2. *For every $s \in (0, T]$, one has $\sigma(s) > 0$. Consequently, $p_s = \text{Law}(X_s)$ admits a strictly positive C^∞ density, and*

$$V_s := -\log p_s \in C^\infty(\mathbb{R}^d).$$

In particular, κ_{V_s} is well defined for every $s > 0$.

Proof. Since $g(u) > 0$ for $u > 0$, the representation

$$\sigma^2(s) = \int_0^s \exp\left(-2 \int_u^s f(v) \, dv\right) g^2(u) \, du$$

has strictly positive integrand, hence $\sigma(s) > 0$ for $s > 0$. Moreover,

$$X_s \stackrel{d}{=} a(s)X_0 + \sigma(s)\xi, \quad \xi \sim \mathcal{N}(0, I_d),$$

so $p_s = (S_{a(s)}p_0) * \mathcal{N}(0, \sigma^2(s)I_d)$. Thus p_s is the convolution of a probability measure with a nondegenerate Gaussian density, hence it is strictly positive and C^∞ . Therefore $V_s = -\log p_s \in C^\infty(\mathbb{R}^d)$. \square

A.2 Profile calculus under OU smoothing

The next bounds package the smoothing mechanism above into the form used later. The scaling lemma isolates what the deterministic factor $a(s)$ does to the profile. The weak-semiconvexity invariance of Gaussian convolution from Conforti [2024, Theorem 2.1] is then applied not to U itself but to $h = U - \frac{\alpha'}{2} \|\cdot\|^2$, because the defect class \mathcal{F}_M is stable only after the explicit quadratic curvature has been separated off. The factorization lemma explains why convolving e^{-U} with a Gaussian becomes a heat flow of e^{-h} evaluated at a rescaled point, multiplied by a new quadratic tilt. That is the precise origin of the denominator $1 + \alpha'\sigma^2$ in the final profile formulas; see also Gentiloni-Silveri and Ocello [2025, Appendix B] for the same input in the diffusion-model setting.

Lemma 3. *For all $M > 0$ and $r \geq 0$,*

$$0 \leq f_M(r) \leq \min\{Mr, 2\sqrt{M}\}.$$

Consequently, for every $r > 0$,

$$\frac{1}{r}f_M(r) \leq \min\left\{M, \frac{2\sqrt{M}}{r}\right\}.$$

Proof. The claim is trivial if $M = 0$ or $r = 0$. Otherwise, with $y = \frac{1}{2}\sqrt{M}r$, one has $f_M(r) = 2\sqrt{M} \tanh(y)$, and $\tanh(y) \leq \min\{y, 1\}$ gives

$$f_M(r) \leq \min\{2\sqrt{M}y, 2\sqrt{M}\} = \min\{Mr, 2\sqrt{M}\}.$$

Dividing by $r > 0$ yields the second bound. \square

For $u > 0$, let γ_u denote the density of $\mathcal{N}(0, uI_d)$, and define

$$(P_u\phi)(x) := \int_{\mathbb{R}^d} \phi(y) \gamma_u(x-y) dy.$$

For $M > 0$, set

$$\mathcal{F}_M := \left\{h \in C^1(\mathbb{R}^d) : \kappa_h(r) \geq -\frac{1}{r}f_M(r) \quad \forall r > 0\right\}.$$

Lemma 4. *Let $p_0 \propto e^{-V_0}$ with $V_0 \in C^1(\mathbb{R}^d)$, and for $a > 0$ let*

$$q := S_a p_0, \quad U_a := -\log q.$$

Then for every $r > 0$,

$$\kappa_{U_a}(r) = \frac{1}{a^2} \kappa_{V_0}(r/a).$$

In particular, if

$$\kappa_{V_0}(r) \geq \alpha - \frac{1}{r}f_M(r), \quad r > 0,$$

then

$$\kappa_{U_a}(r) \geq \frac{\alpha}{a^2} - \frac{1}{r}f_{M/a^2}(r), \quad r > 0.$$

Proof. Since $q(x) = a^{-d}p_0(x/a)$, one has $U_a(x) = V_0(x/a) + \text{const}$ and $\nabla U_a(x) = a^{-1}\nabla V_0(x/a)$. Thus, for $u = x/a, v = y/a$,

$$\frac{\langle \nabla U_a(x) - \nabla U_a(y), x - y \rangle}{\|x - y\|^2} = \frac{1}{a^2} \frac{\langle \nabla V_0(u) - \nabla V_0(v), u - v \rangle}{\|u - v\|^2}.$$

Taking the infimum over $\|x - y\| = r$, equivalently $\|u - v\| = r/a$, gives the first identity. The second follows by applying the assumed lower bound at radius r/a and using $a^{-1}f_M(r/a) = f_{M/a^2}(r)$. \square

Lemma 5 (Heat semigroup invariance of \mathcal{F}_M). *Let $M > 0$ and $h \in \mathcal{F}_M$. For $u > 0$, define*

$$H_u(x) := -\log(P_u(e^{-h}))(x).$$

Then $H_u \in \mathcal{F}_M$.

Proof. This is exactly Conforti [2024, Theorem 2.1]. □

Lemma 6. Let $U : \mathbb{R}^d \rightarrow \mathbb{R}$, $\sigma > 0$, and $\alpha' \geq 0$. Define

$$h(y) := U(y) - \frac{\alpha'}{2} \|y\|^2, \quad A := 1 + \alpha' \sigma^2, \quad \tau := \frac{\sigma^2}{A}.$$

Let

$$p(x) := \int_{\mathbb{R}^d} e^{-U(y)} \gamma_{\sigma^2}(x - y) \, dy.$$

Then there exists $C = C(\alpha', \sigma, d)$ such that for all $x \in \mathbb{R}^d$,

$$p(x) = C \exp\left(-\frac{\alpha'}{2A} \|x\|^2\right) \left(P_\tau(e^{-h})\right)\left(\frac{x}{A}\right).$$

Proof. Since $e^{-U(y)} = e^{-h(y)} e^{-\alpha' \|y\|^2/2}$, one gets

$$p(x) = (2\pi\sigma^2)^{-d/2} \int_{\mathbb{R}^d} e^{-h(y)} \exp\left(-\frac{\alpha'}{2} \|y\|^2 - \frac{\|x - y\|^2}{2\sigma^2}\right) \, dy.$$

Completing the square gives

$$\frac{\alpha'}{2} \|y\|^2 + \frac{\|x - y\|^2}{2\sigma^2} = \frac{\alpha'}{2A} \|x\|^2 + \frac{1}{2\tau} \left\|y - \frac{x}{A}\right\|^2.$$

Recognizing the Gaussian density γ_τ yields

$$p(x) = A^{-d/2} \exp\left(-\frac{\alpha'}{2A} \|x\|^2\right) \left(P_\tau(e^{-h})\right)\left(\frac{x}{A}\right),$$

so the claim holds with $C = A^{-d/2}$. □

Lemma 7. Let $\alpha' \geq 0$ and $M' \geq 0$. Assume $q \propto e^{-U}$ with $U \in C^1(\mathbb{R}^d)$ satisfies

$$\kappa_U(r) \geq \alpha' - \frac{1}{r} f_{M'}(r), \quad r > 0.$$

Let $p = q * \gamma_{\sigma^2}$ and $V := -\log p$. Then for all $r > 0$,

$$\kappa_V(r) \geq \frac{\alpha'}{1 + \alpha' \sigma^2} - \frac{1}{r} f_{M'/(1 + \alpha' \sigma^2)}(r).$$

Proof. The proof separates the explicit quadratic curvature from the residual defect. The residual part belongs to a class invariant under Gaussian convolution, while the quadratic part can be tracked exactly by completing the square. Set $A := 1 + \alpha' \sigma^2$, $\tau := \sigma^2/A$, and $h := U - \frac{\alpha'}{2} \|\cdot\|^2$. Then $\kappa_h(r) = \kappa_U(r) - \alpha'$, so $h \in \mathcal{F}_{M'}$. By Lemma 6,

$$V(x) = \frac{\alpha'}{2A} \|x\|^2 + H(x/A) + \text{const}, \quad H := -\log \left(P_\tau(e^{-h})\right).$$

Lemma 5 gives $H \in \mathcal{F}_{M'}$. Using the quadratic contribution and the same scaling computation as in Lemma 4,

$$\kappa_V(r) \geq \frac{\alpha'}{A} + \frac{1}{A^2} \kappa_H(r/A) \geq \frac{\alpha'}{A} - \frac{1}{Ar} f_{M'}(r/A) = \frac{\alpha'}{A} - \frac{1}{r} f_{M'/A^2}(r).$$

□

Corollary 1 (OU smoothing of the weak profile). Assume $p_0 \propto e^{-V_0}$ satisfies Assumption 1 with parameters (α, M) . For $s \in (0, T]$, let

$$p_s = (S_{\alpha(s)} p_0) * \gamma_{\sigma^2(s)}, \quad V_s := -\log p_s.$$

Then for every $r > 0$,

$$\kappa_{V_s}(r) \geq \alpha_s - \frac{1}{r} f_{M_s}(r),$$

where

$$\alpha_s = \frac{\alpha}{a^2(s) + \alpha \sigma^2(s)}, \quad M_s = \frac{M a^2(s)}{(a^2(s) + \alpha \sigma^2(s))^2}.$$

Proof. Let U_s denote the potential of $S_{a(s)}p_0$. Lemma 4 gives

$$\kappa_{U_s}(r) \geq \frac{\alpha}{a^2(s)} - \frac{1}{r} f_{M/a^2(s)}(r).$$

Applying Lemma 7 with $\alpha' = \alpha/a^2(s)$, $M' = M/a^2(s)$, and $\sigma = \sigma(s)$ yields

$$\kappa_{V_s}(r) \geq \frac{\alpha/a^2(s)}{1 + (\alpha/a^2(s))\sigma^2(s)} - \frac{1}{r} f_{\frac{M/a^2(s)}{(1+(\alpha/a^2(s))\sigma^2(s))^2}}(r),$$

which simplifies to the stated formulas for α_s and M_s . \square

Remark 2 (Why α_s and M_s share the same denominator). The common denominator $a^2(s) + \alpha\sigma^2(s)$ is the algebraic signature of one smoothing mechanism acting on two different parts of the profile. The factor $a^2(s)$ comes from transporting the initial geometry through the linear part of the forward dynamics, while the term $\alpha\sigma^2(s)$ is the quadratic curvature that can be fed into the Gaussian-convolution step. The numerators then separate the two roles. The large-scale convex part keeps the factor α , producing α_s , whereas the short-scale defect keeps the factor $M/a^2(s)$, producing M_s . Thus smoothing improves the available convexity and the residual defect through one common denominator, but only the defect remembers how much unsmoothed nonconvexity was still present before convolution.

A.3 Moment consequences

We also need one integrability fact later at switch time. The point is that the defect term in Assumption 1 is uniformly bounded: by Lemma 3, $r^{-1}f_M(r)$ can at worst create a linear loss along rays, while the positive αr term integrates to a quadratic confinement. Thus weak log-concavity with $\alpha > 0$ already forces Gaussian-type tails.

Lemma 8. *Under Assumption 1 with parameters $\alpha, M > 0$, there exists a constant $C_0 < \infty$ such that*

$$V_0(x) \geq \frac{\alpha}{4}\|x\|^2 - C_0, \quad \forall x \in \mathbb{R}^d.$$

Consequently,

$$p_0 \in \mathcal{P}_p(\mathbb{R}^d) \quad \text{for every } p \geq 1.$$

Moreover, all forward marginals $p_s = \text{Law}(X_s)$ also belong to $\mathcal{P}_p(\mathbb{R}^d)$ for every $p \geq 1$.

Proof. Fix $x = ru$ with $r = \|x\| > 0$ and $\|u\| = 1$. Applying Assumption 1 with $y = 0$ gives

$$\langle \nabla V_0(ru) - \nabla V_0(0), u \rangle \geq \alpha r - f_M(r),$$

hence

$$\langle \nabla V_0(ru), u \rangle \geq \alpha r - f_M(r) - \|\nabla V_0(0)\|.$$

Integrating along the ray $s \mapsto su$,

$$V_0(ru) - V_0(0) = \int_0^r \langle \nabla V_0(su), u \rangle ds \geq \frac{\alpha}{2}r^2 - \int_0^r f_M(s) ds - \|\nabla V_0(0)\| r.$$

By Lemma 3, $f_M(s) \leq 2\sqrt{M}$, so

$$V_0(x) \geq V_0(0) + \frac{\alpha}{2}\|x\|^2 - (2\sqrt{M} + \|\nabla V_0(0)\|)\|x\|.$$

Absorbing the linear term into the quadratic term yields $V_0(x) \geq \frac{\alpha}{4}\|x\|^2 - C_0$ for some $C_0 < \infty$. Thus $e^{-V_0(x)} \lesssim e^{-\alpha\|x\|^2/4}$, so p_0 has finite moments of every order. The same then holds for p_s because

$$X_s \stackrel{d}{=} a(s)X_0 + \sigma(s)\xi, \quad \xi \sim \mathcal{N}(0, I_d),$$

and Gaussian moments are finite. \square

B Profile transfer, Euclidean closure, and admissible switches

This section translates the smoothing output into geometry of the learned reverse drift. For each noise level s , the learned reverse drift inherits a radial lower envelope

$$\underline{\kappa}_s(r) = \mathfrak{m}(s) - g^2(s) \frac{1}{r} f_{M_s}(r), \quad r > 0,$$

where $s = T - t$. The key point is that this is one and the same monotone-in- r curve. Its left endpoint is the Euclidean load $-\mathfrak{b}(s)$, which is the quantity seen by synchronous coupling. Its right endpoint is the far-field reserve $\mathfrak{m}(s)$, which is the quantity later converted into contraction by reflection coupling. Thus the later coupling split is not imposed from outside: it is already encoded in the shape of $\underline{\kappa}_s$. No stochastic argument is needed yet; the whole section is deterministic radial bookkeeping.

B.1 One profile, two endpoints

Proof of Lemma 1. Fix $t \in [0, T]$ and write $s := T - t$.

Item (i): profile transfer. For $x \neq y$, set $r := \|x - y\|$. Since

$$\widehat{b}_t(x) = f(s)x + g^2(s)\nabla \log p_s(x) + g^2(s)e_s(x),$$

one has

$$-\frac{\langle \widehat{b}_t(x) - \widehat{b}_t(y), x - y \rangle}{\|x - y\|^2} = -f(s) - g^2(s) \frac{\langle \nabla \log p_s(x) - \nabla \log p_s(y), x - y \rangle}{\|x - y\|^2} - g^2(s) \frac{\langle e_s(x) - e_s(y), x - y \rangle}{\|x - y\|^2}.$$

Because $\nabla \log p_s = -\nabla V_s$, the middle term is $\kappa_{V_s}(r)$. By Corollary 1,

$$\kappa_{V_s}(r) \geq \alpha_s - \frac{1}{r} f_{M_s}(r),$$

and Assumption 3 gives

$$\frac{\langle e_s(x) - e_s(y), x - y \rangle}{\|x - y\|^2} \leq \ell(s).$$

Combining the two bounds yields

$$-\frac{\langle \widehat{b}_t(x) - \widehat{b}_t(y), x - y \rangle}{\|x - y\|^2} \geq g^2(s) \left(\alpha_s - \frac{1}{r} f_{M_s}(r) - \ell(s) \right) - f(s) = \underline{\kappa}_s(r).$$

Taking the infimum over all pairs with $\|x - y\| = r$ proves (20).

Item (ii): endpoint structure of the same profile. Define

$$q_M(r) := \frac{1}{r} f_M(r), \quad r > 0.$$

Then

$$\underline{\kappa}_s(r) = \mathfrak{m}(s) - g^2(s) q_{M_s}(r).$$

If $M_s = 0$, then $f_{M_s} \equiv 0$, so $\underline{\kappa}_s(r) \equiv \mathfrak{m}(s)$, and all claims are immediate. Assume now that $M_s > 0$. With $z = \frac{1}{2} \sqrt{M_s} r$ and $\psi(z) := \tanh(z)/z$, one has

$$q_{M_s}(r) = M_s \psi \left(\frac{1}{2} \sqrt{M_s} r \right).$$

Moreover,

$$\psi'(z) = \frac{z \operatorname{sech}^2(z) - \tanh(z)}{z^2} = -\frac{\tanh(z) - z \operatorname{sech}^2(z)}{z^2}.$$

Set $h(z) := \tanh(z) - z \operatorname{sech}^2(z)$. Then $h(0) = 0$ and

$$h'(z) = 2z \operatorname{sech}^2(z) \tanh(z) \geq 0 \quad (z \geq 0),$$

so $h(z) \geq 0$ for $z \geq 0$. Hence $\psi'(z) \leq 0$, and therefore $r \mapsto q_{M_s}(r)$ is nonincreasing on $(0, \infty)$. Consequently $r \mapsto \underline{\kappa}_s(r)$ is nondecreasing on $(0, \infty)$.

The endpoint limits now follow from

$$\lim_{z \downarrow 0} \frac{\tanh(z)}{z} = 1, \quad \lim_{z \rightarrow \infty} \frac{\tanh(z)}{z} = 0.$$

Indeed,

$$\lim_{r \downarrow 0} q_{M_s}(r) = M_s, \quad \lim_{r \rightarrow \infty} q_{M_s}(r) = 0,$$

hence

$$\lim_{r \downarrow 0} \underline{\kappa}_s(r) = \mathfrak{m}(s) - g^2(s)M_s = -\mathfrak{b}(s),$$

and

$$\lim_{r \rightarrow \infty} \underline{\kappa}_s(r) = \mathfrak{m}(s).$$

The identity is just the rearrangement

$$\mathfrak{m}(s) + \mathfrak{b}(s) = g^2(s)M_s.$$

If $\mathfrak{m}(s) > 0$, the second limit implies that there exists $r_* > 0$ such that $\underline{\kappa}_s(r_*) > 0$. By monotonicity, $\underline{\kappa}_s(r) \geq 0$ for all $r \geq r_*$. Therefore the set in (22) is nonempty, so $R(s) < \infty$, and $\underline{\kappa}_s(r) \geq 0$ for all $r \geq R(s)$.

Item (iii): companion Euclidean load. By item (ii),

$$\underline{\kappa}_s(r) \geq \lim_{u \downarrow 0} \underline{\kappa}_s(u) = -\mathfrak{b}(s), \quad r > 0.$$

Together with item (i), this yields

$$\kappa_{\widehat{b}_t}(r) \geq -\mathfrak{b}(s), \quad r > 0.$$

Hence, for $x \neq y$,

$$\langle x - y, \widehat{b}_t(x) - \widehat{b}_t(y) \rangle \leq -\kappa_{\widehat{b}_t}(\|x - y\|)\|x - y\|^2 \leq \mathfrak{b}(s)\|x - y\|^2.$$

The case $x = y$ is trivial, proving (23). \square

Remark 3 (Geometry behind the later coupling split). Fix $s \in (0, T]$. The curve $r \mapsto \underline{\kappa}_s(r)$ rises from the near-field value $-\mathfrak{b}(s)$ to the far-field value $\mathfrak{m}(s)$. So Euclidean geometry and radial geometry are reading different parts of the same object. A synchronous-coupling estimate for $\|Y_t - \bar{Y}_t\|^2$ collapses the whole curve to its left endpoint, because it must control pairwise separation uniformly over all radii. By contrast, reflection coupling can act directly on the radial process and therefore exploit the fact that the same profile may already be positive in the tail even when its near-field endpoint is still negative. This is exactly the metric-mismatch regime: far-field contraction has appeared, but Euclidean closure has not. The switch metric introduced later is tailored to that shape—it suppresses the near-field defect while keeping sensitivity to the contractive tail.

B.2 Admissible switches

Definition 4 asks that the far-field endpoint stay positive on the whole remaining noise interval. By Remark 3, this does *not* mean that Euclidean geometry has already been restored. It only means that every instantaneous profile on $[s_0, T]$ has a positive tail, which is the minimum robust input needed later to build one time-uniform switch metric and run a single reflection-coupling argument on the whole early window.

Proposition 1 (Structure of the admissible switch set). *Assume that \mathfrak{m} is continuous on $(0, T]$. Then the map*

$$s_0 \mapsto \underline{\mathfrak{m}}(s_0) := \inf_{u \in [s_0, T]} \mathfrak{m}(u)$$

is nondecreasing and continuous on $(0, T]$. Consequently,

$$\mathcal{S}_{\text{adm}} = \{s_0 \in (0, T] : \underline{\mathfrak{m}}(s_0) > 0\}$$

is an upper interval of $(0, T]$. If, in addition, $\mathfrak{m}(T) > 0$, then a nontrivial admissible switch exists. Moreover, if $s_{\min} := \inf \mathcal{S}_{\text{adm}} \in (0, T)$, then

$$\mathfrak{m}(s_{\min}) = 0.$$

Proof. If $0 < s_1 \leq s_2 \leq T$, then $[s_2, T] \subseteq [s_1, T]$, hence

$$\underline{m}(s_1) = \inf_{u \in [s_1, T]} \mathbf{m}(u) \leq \inf_{u \in [s_2, T]} \mathbf{m}(u) = \underline{m}(s_2),$$

so $s_0 \mapsto \underline{m}(s_0)$ is nondecreasing.

To prove continuity, define

$$F(s_0, \theta) := \mathbf{m}((1 - \theta)s_0 + \theta T), \quad (s_0, \theta) \in (0, T] \times [0, 1].$$

Since \mathbf{m} is continuous, so is F , and

$$\underline{m}(s_0) = \min_{\theta \in [0, 1]} F(s_0, \theta).$$

The minimum of a continuous function over the compact set $[0, 1]$ depends continuously on s_0 , hence \underline{m} is continuous on $(0, T]$.

Because $\mathcal{S}_{\text{adm}} = \underline{m}^{-1}((0, \infty))$ and \underline{m} is nondecreasing, \mathcal{S}_{adm} is an upper interval. If $\mathbf{m}(T) > 0$, continuity gives $\eta > 0$ such that $\mathbf{m}(u) > 0$ on $[T - \eta, T]$, hence $\underline{m}(T - \eta) > 0$, so a nontrivial admissible switch exists. Finally, let $s_{\min} := \inf \mathcal{S}_{\text{adm}} \in (0, T)$. Since \mathcal{S}_{adm} is an upper interval, every $u > s_{\min}$ belongs to \mathcal{S}_{adm} , hence

$$\underline{m}(u) > 0, \quad u \in (s_{\min}, T].$$

Therefore, for every $u > s_{\min}$ and every $r \in [u, T]$,

$$\mathbf{m}(r) \geq \underline{m}(u) > 0.$$

As $u > s_{\min}$ is arbitrary, this implies

$$\mathbf{m}(r) > 0, \quad r \in (s_{\min}, T].$$

Suppose, for contradiction, that $\mathbf{m}(s_{\min}) > 0$. Then continuity of \mathbf{m} implies that \mathbf{m} is strictly positive on the compact interval $[s_{\min}, T]$, so

$$\underline{m}(s_{\min}) = \min_{u \in [s_{\min}, T]} \mathbf{m}(u) > 0.$$

By continuity of \underline{m} , there exists $\eta > 0$ such that

$$\underline{m}(s_{\min} - \eta) > 0,$$

contradicting the definition of s_{\min} . Thus $\mathbf{m}(s_{\min}) = 0$. \square

Remark 4 (Why admissibility is the right threshold for the next section). Admissibility is intentionally weaker than Euclidean stability. It does not require $\mathbf{b}(u) \leq 0$ on $[s_0, T]$, so one cannot generally replace the early radial route by a direct W_2 argument on that whole window. What it guarantees instead is that the positive tail survives uniformly after taking the infimum over $u \in [s_0, T]$. The next section turns exactly that surviving tail positivity into a two-zone lower envelope with a bounded near-field loss and a strictly positive far-field reserve.

Remark 5 (The radial portrait in the main text is schematic). Figure 1 should be read as a pointwise visualization of the lower profile $(s, r) \mapsto \underline{\kappa}_s(r)$. The threshold radius $R(s)$ is only an instantaneous zero-crossing scale. Later we will replace it by the switch-dependent radius $R_{\text{sw}}(s_0)$, which is a uniform envelope radius on the whole early window rather than a pointwise radius at a single s . No claim is made here that $R(s)$ moves monotonically inward with the noise level.

C Early-phase damping in the switch metric

Fix a grid-aligned admissible switch $s_0 \in \mathcal{S}_{\text{adm}}$, and write

$$t_s := T - s_0 = t_K.$$

This section proves the early-window contraction used later. The proof has three steps: build a time-uniform switch-level lower envelope on $[0, t_s]$; use reflection coupling only for two copies of the learned reverse SDE to obtain semigroup contraction in $W_{\varphi_{s_0}}$; and insert the three pre-switch

error channels (initialization, discretization, and score forcing) at their entry times and propagate them to t_s under that contraction.

Two couplings appear and should not be conflated. Reflection coupling is used only to prove the learned-semigroup contraction. When comparing the ideal and learned reverse SDEs over a short interval, we instead use synchronous coupling, so the common noise cancels and only the drift mismatch δ_t remains. Throughout this section, $P_{u,v}$ denotes the exact learned reverse semigroup on $[u, v]$, $P_k := P_{t_k, t_{k+1}}$ the exact learned one-step kernels, and Ψ_k the numerical one-step kernels; we write

$$\delta_t(x) := \widehat{b}_t(x) - b_t(x) = g^2(T-t)e_{T-t}(x). \quad (28)$$

Whenever Lemma 13 is invoked, we additionally use the theorem-level input stated there: strong well posedness of the learned reverse SDE on $[0, t_s]$, existence of coalescing reflection couplings on every subinterval, and the finiteness conditions $\underline{g}(s_0) > 0$, $\bar{\mathfrak{b}}(s_0) < \infty$, and $\overline{G}(s_0) < \infty$.

Whenever Lemma 14 is invoked, we also use the theorem-level existence of a global ideal reverse solution

$$(\tilde{X}_t)_{0 \leq t \leq T}$$

to (12) with

$$\text{Law}(\tilde{X}_t) = p_{T-t}, \quad 0 \leq t \leq T.$$

C.1 From admissibility to a uniform early profile

The first deliberate loss of information occurs here. We replace the full family $(r \mapsto \underline{\kappa}_s(r))_{s \in [s_0, T]}$ by a switch-dependent two-zone lower envelope: a bounded near-field load and a strictly positive far-field reserve. This loses the detailed radius dependence of the exact profile, but gains the uniformity in t needed by the later coupling argument.

Define

$$\underline{g}(s_0) := \inf_{u \in [s_0, T]} g(u), \quad \bar{\mathfrak{b}}(s_0) := \sup_{u \in [s_0, T]} \mathfrak{b}(u), \quad \overline{G}(s_0) := \sup_{u \in [s_0, T]} g^2(u) \sqrt{M_u},$$

$$R_{\text{sw}}(s_0) := \frac{4\overline{G}(s_0)}{\underline{m}(s_0)}, \quad m_{\text{sw}}(s_0) := \frac{\underline{m}(s_0)}{2}.$$

Here $R_{\text{sw}}(s_0)$ is a switch-dependent uniform envelope radius on the whole early window; it is not the instantaneous zero-crossing radius $R(s)$ from (22). Define the switch-level lower profile

$$\underline{\kappa}_{s_0}(r) := \begin{cases} -\bar{\mathfrak{b}}(s_0), & 0 < r \leq R_{\text{sw}}(s_0), \\ m_{\text{sw}}(s_0), & r > R_{\text{sw}}(s_0). \end{cases}$$

Lemma 9. Fix $s_0 \in \mathcal{S}_{\text{adm}}$ and assume $\bar{\mathfrak{b}}(s_0) < \infty$ and $\overline{G}(s_0) < \infty$. Then for every $t \in [0, t_s]$ and every $r > 0$,

$$\kappa_{\widehat{b}_t}(r) \geq \underline{\kappa}_{s_0}(r), \quad (29)$$

and

$$g(T-t) \geq \underline{g}(s_0). \quad (30)$$

Proof. Fix $t \in [0, t_s]$ and set $s := T-t \in [s_0, T]$. By Lemma 1(i),

$$\kappa_{\widehat{b}_t}(r) \geq \underline{\kappa}_s(r) = \mathfrak{m}(s) - g^2(s) \frac{1}{r} f_{M_s}(r), \quad r > 0.$$

If $0 < r \leq R_{\text{sw}}(s_0)$, then Lemma 3 gives $r^{-1} f_{M_s}(r) \leq M_s$, hence

$$\kappa_{\widehat{b}_t}(r) \geq g^2(s)(\alpha_s - \ell(s) - M_s) - f(s) = -\mathfrak{b}(s) \geq -\bar{\mathfrak{b}}(s_0).$$

If $r > R_{\text{sw}}(s_0)$, then Lemma 3 gives $f_{M_s}(r) \leq 2\sqrt{M_s}$, and therefore

$$\kappa_{\widehat{b}_t}(r) \geq \mathfrak{m}(s) - \frac{2g^2(s)\sqrt{M_s}}{r} \geq \underline{m}(s_0) - \frac{2\overline{G}(s_0)}{r}.$$

By the definition of $R_{\text{sw}}(s_0)$, the last term is bounded below by

$$\underline{m}(s_0) - \frac{2\overline{G}(s_0)}{R_{\text{sw}}(s_0)} = \frac{\underline{m}(s_0)}{2} = m_{\text{sw}}(s_0).$$

This proves (29). The bound (30) is immediate from the definition of $\underline{g}(s_0)$. \square

C.2 Reflection coupling and radial reduction

With the uniform profile in hand, the problem becomes one-dimensional. For two copies of the learned reverse SDE, reflection coupling is the natural choice because it puts the stochastic forcing entirely in the radial direction of the separation vector. The distance process then sees the drift only through the scalar profile $\kappa_{\widehat{b}_t}(r_t)$, exactly the object extracted in the previous subsection.

Definition 5 (Coalescing reflection coupling). Fix $0 \leq t_1 < t_2 \leq t_s$. Let Y and \bar{Y} be solutions of the learned reverse SDE (13) on $[t_1, t_2]$, defined on a common filtered probability space. Set

$$D_t := Y_t - \bar{Y}_t, \quad r_t := \|D_t\|, \quad \tau_c := \inf\{t \geq t_1 : r_t = 0\}.$$

Fix a deterministic unit vector $e \in \mathbb{R}^d$, and define

$$n_t := \frac{D_t}{r_t} \mathbf{1}_{\{r_t > 0\}} + e \mathbf{1}_{\{r_t = 0\}}, \quad H_t := (I_d - 2n_t n_t^\top) \mathbf{1}_{\{t < \tau_c\}} + I_d \mathbf{1}_{\{t \geq \tau_c\}}.$$

If Y is driven by a Brownian motion \bar{B} , define

$$\bar{B}_t^{\text{ref}} := \int_{t_1}^t H_u \, d\bar{B}_u.$$

The pair (Y, \bar{Y}) is said to be in *coalescing reflection coupling* if Y is driven by \bar{B} and \bar{Y} is driven by \bar{B}^{ref} . Since $H_t H_t^\top = I_d$, Lévy's characterization implies that \bar{B}^{ref} is again a Brownian motion. After τ_c , both copies evolve synchronously and therefore stick together.

Lemma 10 (Radial dynamics under reflection coupling). Fix $s_0 \in \mathcal{S}_{\text{adm}}$, and let Y, \bar{Y} be coupled as in Definition 5 on $[t_1, t_2] \subseteq [0, t_s]$. Then there exists a one-dimensional Brownian motion W such that, for $t < \tau_c$,

$$dr_t = \left\langle \frac{D_t}{\|D_t\|}, \widehat{b}_t(Y_t) - \widehat{b}_t(\bar{Y}_t) \right\rangle dt + 2g(T-t) \, dW_t. \quad (31)$$

Moreover,

$$\left\langle \frac{D_t}{\|D_t\|}, \widehat{b}_t(Y_t) - \widehat{b}_t(\bar{Y}_t) \right\rangle \leq -\kappa_{\widehat{b}_t}(r_t) r_t, \quad (32)$$

and hence

$$dr_t \leq -\underline{\kappa}_{s_0}(r_t) r_t \, dt + 2g(T-t) \, dW_t, \quad t < \tau_c. \quad (33)$$

Proof. For $t < \tau_c$, one has $n_t = D_t/r_t$ and

$$I_d - H_t = 2n_t n_t^\top.$$

Hence

$$dD_t = (\widehat{b}_t(Y_t) - \widehat{b}_t(\bar{Y}_t)) \, dt + 2g(T-t) n_t n_t^\top \, d\bar{B}_t = (\widehat{b}_t(Y_t) - \widehat{b}_t(\bar{Y}_t)) \, dt + 2g(T-t) n_t \, dW_t,$$

where

$$W_t - W_{t_1} := \int_{t_1}^t \langle n_u, d\bar{B}_u \rangle.$$

Since n_t is predictable and $\|n_t\| = 1$ on $\{t < \tau_c\}$, W is a one-dimensional Brownian motion.

To justify the radial equation, localize away from the origin. For $n \geq 1$, let

$$\tau_n := \inf\{t \geq t_1 : r_t \leq n^{-1}\}.$$

On $[t_1, \tau_n]$, the map $x \mapsto \|x\|$ is C^2 in a neighborhood of D_t , so Itô's formula gives

$$dr_t = \left\langle \frac{D_t}{\|D_t\|}, \widehat{b}_t(Y_t) - \widehat{b}_t(\bar{Y}_t) \right\rangle dt + 2g(T-t) \, dW_t + \frac{1}{2} \text{Tr}(4g(T-t)^2 n_t n_t^\top \nabla^2 \|D_t\|) \, dt.$$

Now

$$\nabla^2 \|x\| = \frac{1}{\|x\|} \left(I_d - \frac{xx^\top}{\|x\|^2} \right), \quad x \neq 0,$$

and $n_t = D_t/\|D_t\|$, so

$$\text{Tr}(n_t n_t^\top \nabla^2 \|D_t\|) = 0.$$

Thus the second-order term vanishes identically. Letting $n \rightarrow \infty$ proves (31) for $t < \tau_c$.

The bound (32) is immediate from Definition 2, because $r_t = \|D_t\|$. Combining it with Lemma 9 gives (33). \square

C.3 The switch metric as a radial Lyapunov gauge

Definition 6 (Radial-cost Wasserstein metric). Let $\varphi : [0, \infty) \rightarrow [0, \infty)$ be increasing, concave, and satisfy $\varphi(0) = 0$. For $\mu, \nu \in \mathcal{P}_1(\mathbb{R}^d)$, define

$$W_\varphi(\mu, \nu) := \inf_{\pi \in \Pi(\mu, \nu)} \int_{\mathbb{R}^d \times \mathbb{R}^d} \varphi(\|x - y\|) \pi(dx, dy).$$

For such φ , the concavity and monotonicity of φ imply subadditivity, and the usual gluing argument shows that W_φ is a transport metric on $\mathcal{P}_1(\mathbb{R}^d)$.

The remaining task is to choose a concave cost whose generator absorbs the two-zone radial inequality from Lemma 9. On the core $[0, R_{\text{sw}}(s_0)]$, the drift may still expand, so one needs negative curvature of φ to be paid for by the diffusion term. Beyond $R_{\text{sw}}(s_0)$, the drift is already uniformly contractive, so further concavity would only waste this reserve. This leads to a Gaussian core and an affine tail.

For the fixed switch s_0 , define

$$\lambda(s_0) := \frac{\bar{\mathbf{b}}(s_0)^+ + m_{\text{sw}}(s_0)}{4g(s_0)^2}, \quad \mathbf{a}(s_0) := e^{-\lambda(s_0)R_{\text{sw}}(s_0)^2}, \quad c(s_0) := m_{\text{sw}}(s_0)\mathbf{a}(s_0). \quad (34)$$

Attach to s_0 the cost

$$\varphi_{s_0}(r) := \begin{cases} \int_0^r e^{-\lambda(s_0)u^2} du, & 0 \leq r \leq R_{\text{sw}}(s_0), \\ \varphi_{s_0}(R_{\text{sw}}(s_0)) + \mathbf{a}(s_0)(r - R_{\text{sw}}(s_0)), & r \geq R_{\text{sw}}(s_0). \end{cases} \quad (35)$$

Lemma 11 (The switch gauge and its generator inequality). Fix $s_0 \in \mathcal{S}_{\text{adm}}$ such that $g(s_0) > 0$, $\bar{\mathbf{b}}(s_0) < \infty$, and $\bar{G}(s_0) < \infty$. Then $\varphi_{s_0} \in C^1([0, \infty))$ is increasing and concave, and for all $r \geq 0$,

$$\mathbf{a}(s_0)r \leq \varphi_{s_0}(r) \leq r. \quad (36)$$

Moreover,

$$2g(s_0)^2\varphi_{s_0}''(r) - \underline{\kappa}_{s_0}(r)r\varphi_{s_0}'(r) \leq -c(s_0)\varphi_{s_0}(r) \quad \text{for a.e. } r > 0. \quad (37)$$

Consequently, $W_{\varphi_{s_0}}$ is finite on $\mathcal{P}_1(\mathbb{R}^d)$ and satisfies the triangle inequality.

Proof. For brevity write

$$\begin{aligned} \lambda &:= \lambda(s_0), & R &:= R_{\text{sw}}(s_0), & g &:= g(s_0), & \bar{\mathbf{b}} &:= \bar{\mathbf{b}}(s_0), & m &:= m_{\text{sw}}(s_0), \\ \mathbf{a} &:= \mathbf{a}(s_0), & c &:= c(s_0), & \underline{\kappa} &:= \underline{\kappa}_{s_0}, & \varphi &:= \varphi_{s_0}. \end{aligned}$$

From the definition,

$$\varphi'(r) = \begin{cases} e^{-\lambda r^2}, & 0 < r < R, \\ e^{-\lambda R^2}, & r > R, \end{cases} \quad \varphi''(r) = \begin{cases} -2\lambda r e^{-\lambda r^2}, & 0 < r < R, \\ 0, & r > R, \end{cases}$$

for a.e. $r > 0$. Hence φ is increasing and concave, and φ' is continuous at R , so $\varphi \in C^1([0, \infty))$.

The upper bound $\varphi(r) \leq r$ follows from $0 \leq \varphi' \leq 1$. For the lower bound, if $0 \leq r \leq R$, then

$$\varphi(r) = \int_0^r e^{-\lambda u^2} du \geq r e^{-\lambda R^2} = \mathbf{a}r.$$

If $r \geq R$, then

$$\varphi(r) = \varphi(R) + \mathbf{a}(r - R) \geq \mathbf{a}R + \mathbf{a}(r - R) = \mathbf{a}r.$$

This proves (36).

If $0 < r \leq R$, then $\underline{\kappa}(r) = -\bar{\mathbf{b}}$, and therefore

$$2g^2\varphi''(r) - \underline{\kappa}(r)r\varphi'(r) = (\bar{\mathbf{b}} - 4g^2\lambda)re^{-\lambda r^2}.$$

By the definition of λ ,

$$\bar{\mathbf{b}} - 4g^2\lambda = \bar{\mathbf{b}} - \bar{\mathbf{b}}^+ - m \leq -m.$$

Hence

$$2\underline{g}^2 \varphi''(r) - \underline{\kappa}(r)r\varphi'(r) \leq -mre^{-\lambda r^2}.$$

Since $r \leq R$ implies $e^{-\lambda r^2} \geq e^{-\lambda R^2} = \mathbf{a}$, and $\varphi(r) \leq r$,

$$c\varphi(r) = m\mathbf{a}\varphi(r) \leq me^{-\lambda r^2}r.$$

Thus the generator inequality holds on $(0, R]$.

If $r > R$, then $\underline{\kappa}(r) = m$, $\varphi''(r) = 0$, and $\varphi'(r) = \mathbf{a}$, so

$$2\underline{g}^2 \varphi''(r) - \underline{\kappa}(r)r\varphi'(r) = -m\mathbf{a}r = -cr \leq -c\varphi(r),$$

again because $\varphi(r) \leq r$. This proves (37). \square

C.4 Early semigroup contraction

Remark 6 (The extra theorem-level input used in the early phase). Beyond Assumptions 1–2, the next proposition uses one additional theorem-level input: the learned reverse SDE must be strongly well posed on $[0, t_s]$ and must admit coalescing reflection couplings on each subinterval for every initial coupling. This is not automatic from the standing assumptions. Later, Proposition 7 and Corollary 4 give convenient sufficient conditions, including the standard global/local Lipschitz regimes used in the literature.

Lemma 12 (Signed-load Grönwall for synchronized differences). *Let $D : [u, v] \rightarrow \mathbb{R}^d$ be absolutely continuous. Assume that $\beta \in L^1(u, v)$, $F \in L^1(u, v; \mathbb{R}^d)$, and for a.e. $t \in [u, v]$,*

$$\dot{D}_t = A_t + F_t, \quad \langle D_t, A_t \rangle \leq \beta(t)\|D_t\|^2.$$

Then for every $t \in [u, v]$,

$$\|D_t\| \leq e^{\int_u^t \beta(r) dr} \|D_u\| + \int_u^t e^{\int_r^t \beta(\tau) d\tau} \|F_r\| dr.$$

Proof. For $\varepsilon > 0$, define

$$q_\varepsilon(t) := \sqrt{\|D_t\|^2 + \varepsilon}.$$

Since D is absolutely continuous, so is q_ε , and for a.e. t ,

$$q'_\varepsilon(t) = \frac{\langle D_t, A_t + F_t \rangle}{q_\varepsilon(t)} \leq \beta(t) \frac{\|D_t\|^2}{q_\varepsilon(t)} + \|F_t\|.$$

Now

$$\beta(t) \frac{\|D_t\|^2}{q_\varepsilon(t)} = \beta(t)q_\varepsilon(t) - \beta(t) \frac{\varepsilon}{q_\varepsilon(t)} \leq \beta(t)q_\varepsilon(t) + |\beta(t)|\sqrt{\varepsilon},$$

because $q_\varepsilon(t) \geq \sqrt{\varepsilon}$. Hence

$$q'_\varepsilon(t) \leq \beta(t)q_\varepsilon(t) + \|F_t\| + |\beta(t)|\sqrt{\varepsilon}.$$

Gronwall's inequality yields

$$q_\varepsilon(t) \leq e^{\int_r^t \beta(\tau) d\tau} q_\varepsilon(u) + \int_u^t e^{\int_r^t \beta(\tau) d\tau} \|F_r\| dr + \sqrt{\varepsilon} \int_u^t e^{\int_r^t \beta(\tau) d\tau} |\beta(r)| dr.$$

Letting $\varepsilon \downarrow 0$ proves the claim. \square

Lemma 13. *Fix $s_0 \in \mathcal{S}_{\text{adm}}$ such that $g(s_0) > 0$, $\bar{\mathbf{b}}(s_0) < \infty$, and $\bar{G}(s_0) < \infty$. Assume, in addition, that the learned reverse SDE is strongly well posed on $[0, t_s]$ and admits coalescing reflection couplings on every subinterval $[u, v] \subseteq [0, t_s]$ for every initial coupling $\pi \in \Pi(\mu, \nu)$ with $\mu, \nu \in \mathcal{P}_1(\mathbb{R}^d)$. Then*

$$W_{\varphi_{s_0}}(\mu P_{u,v}, \nu P_{u,v}) \leq e^{-c(s_0)(v-u)} W_{\varphi_{s_0}}(\mu, \nu), \quad 0 \leq u \leq v \leq t_s, \quad (38)$$

for every $\mu, \nu \in \mathcal{P}_1(\mathbb{R}^d)$.

Proof. Fix $\mu, \nu \in \mathcal{P}_1(\mathbb{R}^d)$ and $0 \leq u \leq v \leq t_s$. Choose any coupling $\pi \in \Pi(\mu, \nu)$, and let (Y_t, \bar{Y}_t) be a coalescing reflection coupling of the learned reverse SDE on $[u, v]$ in the sense of Definition 5, with initial law π . Write

$$r_t := \|Y_t - \bar{Y}_t\|, \quad \varphi := \varphi_{s_0}, \quad c := c(s_0), \quad \underline{g} := \underline{g}(s_0).$$

By Lemma 10,

$$dr_t \leq -\underline{\kappa}_{s_0}(r_t) r_t dt + 2g(T-t) dW_t \quad \text{for } t < \tau_c.$$

Apply Meyer–Itô’s formula to the stopped process $t \mapsto \varphi(r_{t \wedge \tau_c})$. This is legitimate because $\varphi \in C^1$ and is piecewise C^2 , and the only potential local-time term at the gluing point $R_{\text{sw}}(s_0)$ vanishes because φ' is continuous there. Using $\varphi'' \leq 0$ and (33), we obtain

$$d\varphi(r_{t \wedge \tau_c}) \leq \left(2g(T-t)^2 \varphi''(r_t) - \underline{\kappa}_{s_0}(r_t) r_t \varphi'(r_t) \right) \mathbf{1}_{\{t < \tau_c\}} dt + 2g(T-t) \varphi'(r_t) \mathbf{1}_{\{t < \tau_c\}} dW_t.$$

Since $g(T-t) \geq \underline{g}$ on $[u, v]$ and $\varphi'' \leq 0$,

$$2g(T-t)^2 \varphi''(r_t) \leq 2\underline{g}^2 \varphi''(r_t).$$

Hence Lemma 11 gives

$$d\varphi(r_{t \wedge \tau_c}) \leq -c \varphi(r_{t \wedge \tau_c}) dt + 2g(T-t) \varphi'(r_t) \mathbf{1}_{\{t < \tau_c\}} dW_t.$$

Because $0 \leq \varphi' \leq 1$ and $\int_u^v g(T-t)^2 dt < \infty$, the stochastic integral is square integrable and therefore a true martingale. Multiplying by e^{ct} , integrating from u to v , and taking expectations yields

$$\mathbb{E}[\varphi(r_v)] \leq e^{-c(v-u)} \mathbb{E}[\varphi(r_u)].$$

Since the law of (Y_v, \bar{Y}_v) is a coupling of $\mu P_{u,v}$ and $\nu P_{u,v}$,

$$W_\varphi(\mu P_{u,v}, \nu P_{u,v}) \leq \mathbb{E}[\varphi(r_v)] \leq e^{-c(v-u)} \mathbb{E}[\varphi(r_u)].$$

Taking the infimum over $\pi \in \Pi(\mu, \nu)$ proves (38). \square

Once semigroup contraction is available, every pre-switch error source is handled in the same way: insert the error at the time it enters the chain and propagate it to t_s with the damping factor $e^{-c(s_0)(t_s - \cdot)}$. The next proposition separates the three places where error enters: initialization, discretization, and score forcing.

Remark 7 (Why the coupling changes). For the learned reverse SDE, synchronous coupling only sees the near-field endpoint $\mathfrak{b}(s)$, because formally

$$\frac{1}{2} \frac{d}{dt} \|Y_t - \bar{Y}_t\|^2 \leq \mathfrak{b}(s) \|Y_t - \bar{Y}_t\|^2.$$

Reflection coupling instead acts on the radial process and therefore accesses the full profile $r \mapsto \kappa_{\widehat{b}_t}(r)$, including its contractive tail. This is the only reason the proof switches couplings.

Lemma 14. Fix $s_0 \in \mathcal{S}_{\text{adm}}$ with $t_K = t_s := T - s_0$, and assume \widehat{p}_T belongs to $\mathcal{P}_1(\mathbb{R}^d)$, Assumption 2, the hypotheses of Lemma 13, and that the theorem-level ideal reverse SDE (12) admits a global strong solution

$$(\widetilde{X}_t)_{0 \leq t \leq T}$$

with

$$\text{Law}(\widetilde{X}_t) = p_{T-t}, \quad 0 \leq t \leq T.$$

Then

$$\Delta_\varphi^{\text{sw}}(s_0) := W_{\varphi_{s_0}}(\text{Law}(Z_{t_s}), p_{s_0})$$

satisfies

$$\begin{aligned} \Delta_\varphi^{\text{sw}}(s_0) \leq & e^{-c(s_0)t_s} W_{\varphi_{s_0}}(\widehat{p}_T, p_T) + \sum_{k=0}^{K-1} e^{-c(s_0)(t_s - t_{k+1})} \left(\mathbb{E}[\xi_k(Z_{t_k})^2] \right)^{1/2} \\ & + \int_{s_0}^T e^{-c(s_0)(s - s_0)} g^2(s) \varepsilon(s) ds. \end{aligned} \quad (39)$$

In particular, the right-hand side is exactly $\overline{\Delta}_\varphi^{\text{sw}}(s_0)$ from (27).

Proof. Let $\varphi := \varphi_{s_0}$ and $c := c(s_0)$. Write

$$\mu_k := \text{Law}(Z_{t_k}), \quad \rho_k := \mu_k P_{t_k, t_s}, \quad k = 0, \dots, K.$$

Then

$$\rho_0 = \widehat{p}_T P_{0, t_s}, \quad \rho_K = \text{Law}(Z_{t_s}).$$

Initialization mismatch. By Lemma 13,

$$W_\varphi(\widehat{p}_T P_{0, t_s}, p_T P_{0, t_s}) \leq e^{-ct_s} W_\varphi(\widehat{p}_T, p_T).$$

Early discretization. By the triangle inequality for W_φ ,

$$W_\varphi(\rho_K, \rho_0) \leq \sum_{k=0}^{K-1} W_\varphi(\rho_{k+1}, \rho_k).$$

Since

$$\rho_{k+1} = (\mu_k \Psi_k) P_{t_{k+1}, t_s}, \quad \rho_k = (\mu_k P_k) P_{t_{k+1}, t_s},$$

Lemma 13 gives

$$W_\varphi(\rho_{k+1}, \rho_k) \leq e^{-c(t_s - t_{k+1})} W_\varphi(\mu_k \Psi_k, \mu_k P_k).$$

Now $\varphi(r) \leq r$, so $W_\varphi \leq W_1 \leq W_2$. Apply Zhang [2013, Theorem 1.1] on the parameter space $(\mathbb{R}^d, \mathcal{B}(\mathbb{R}^d), \mu_k)$ with

$$\mu_x := \Psi_k(x, \cdot), \quad \nu_x := P_k(x, \cdot), \quad c(y, z) := \|y - z\|^2.$$

This yields a Borel measurable family

$$x \mapsto \pi_k^x \in \Pi(\Psi_k(x, \cdot), P_k(x, \cdot))$$

of optimal couplings for the quadratic cost. Integrating π_k^x against $\mu_k(dx)$ gives a coupling of $\mu_k \Psi_k$ and $\mu_k P_k$, and therefore

$$W_2^2(\mu_k \Psi_k, \mu_k P_k) \leq \int_{\mathbb{R}^d} W_2^2(\Psi_k(x, \cdot), P_k(x, \cdot)) \mu_k(dx) \leq \mathbb{E}[\xi_k(Z_{t_k})^2].$$

Hence

$$W_\varphi(\mu_k \Psi_k, \mu_k P_k) \leq W_2(\mu_k \Psi_k, \mu_k P_k) \leq \left(\mathbb{E}[\xi_k(Z_{t_k})^2] \right)^{1/2}.$$

Summing over k gives

$$W_\varphi(\text{Law}(Z_{t_s}), \widehat{p}_T P_{0, t_s}) \leq \sum_{k=0}^{K-1} e^{-c(t_s - t_{k+1})} \left(\mathbb{E}[\xi_k(Z_{t_k})^2] \right)^{1/2}. \quad (40)$$

Pre-switch score forcing. This step uses two different couplings. To propagate a law discrepancy from time u_{j+1} to t_s , we use the learned-semigroup contraction from Lemma 13, whose proof is based on reflection coupling. But to compare the ideal and learned reverse dynamics on the short interval $[u_j, u_{j+1}]$, we use a synchronous comparison built from the *global* ideal reverse path. No separate restart assumption for the ideal equation is used: we simply restrict the theorem-level solution $(\widetilde{X}_t)_{0 \leq t \leq T}$ of (12) to the interval $[u_j, u_{j+1}]$, and solve the learned equation on the same filtered space and with the same Brownian motion \widetilde{B} , started from the random state \widetilde{X}_{u_j} .

Let $0 = u_0 < \dots < u_m = t_s$ be a partition, and define

$$\eta_j := p_{T-u_j} P_{u_j, t_s}, \quad j = 0, \dots, m.$$

Then $\eta_0 = p_T P_{0, t_s}$ and $\eta_m = p_{s_0}$, so

$$W_\varphi(p_T P_{0, t_s}, p_{s_0}) \leq \sum_{j=0}^{m-1} W_\varphi(\eta_j, \eta_{j+1}).$$

Fix j . Let $Y^{(j)}$ be the strong solution of the learned reverse SDE on $[u_j, u_{j+1}]$, driven by the same Brownian motion \bar{B} as \tilde{X} , and initialized by

$$Y_{u_j}^{(j)} = \tilde{X}_{u_j}.$$

Since $\text{Law}(\tilde{X}_{u_j}) = p_{T-u_j}$, the Markov property of the learned reverse semigroup gives

$$\text{Law}(Y_{u_{j+1}}^{(j)} \mid \mathcal{F}_{u_j}) = P_{u_j, u_{j+1}}(\tilde{X}_{u_j}, \cdot),$$

and therefore

$$\text{Law}(Y_{u_{j+1}}^{(j)}) = p_{T-u_j} P_{u_j, u_{j+1}}.$$

On the other hand, because \tilde{X} is the global ideal reverse trajectory,

$$\text{Law}(\tilde{X}_{u_{j+1}}) = p_{T-u_{j+1}}.$$

Therefore

$$\eta_j = \text{Law}(Y_{u_{j+1}}^{(j)}) P_{u_{j+1}, t_s}, \quad \eta_{j+1} = \text{Law}(\tilde{X}_{u_{j+1}}) P_{u_{j+1}, t_s}.$$

Applying Lemma 13 from u_{j+1} to t_s gives

$$W_\varphi(\eta_j, \eta_{j+1}) \leq e^{-c(t_s - u_{j+1})} W_\varphi(\text{Law}(Y_{u_{j+1}}^{(j)}), \text{Law}(\tilde{X}_{u_{j+1}})).$$

Set $D_t := Y_t^{(j)} - \tilde{X}_t$. Because the Brownian motions are identical, the noise cancels and

$$\dot{D}_t = \hat{b}_t(Y_t^{(j)}) - \hat{b}_t(\tilde{X}_t) + \delta_t(\tilde{X}_t) \quad \text{for a.e. } t \in [u_j, u_{j+1}].$$

By Lemma 1(iii),

$$\langle D_t, \hat{b}_t(Y_t^{(j)}) - \hat{b}_t(\tilde{X}_t) \rangle \leq \mathbf{b}(T-t) \|D_t\|^2 \leq \bar{\mathbf{b}}(s_0) \|D_t\|^2$$

for a.e. $t \in [u_j, u_{j+1}]$. Lemma 12, with

$$A_t := \hat{b}_t(Y_t^{(j)}) - \hat{b}_t(\tilde{X}_t), \quad F_t := \delta_t(\tilde{X}_t), \quad \beta(t) := \bar{\mathbf{b}}(s_0),$$

and $D_{u_j} = 0$, therefore yields

$$\|D_{u_{j+1}}\| \leq \int_{u_j}^{u_{j+1}} e^{\bar{\mathbf{b}}(s_0)(u_{j+1}-r)} \|\delta_r(\tilde{X}_r)\| \, dr.$$

Since $W_\varphi \leq W_1$, the coupling $(Y_{u_{j+1}}^{(j)}, \tilde{X}_{u_{j+1}})$ gives

$$W_\varphi(\text{Law}(Y_{u_{j+1}}^{(j)}), \text{Law}(\tilde{X}_{u_{j+1}})) \leq \mathbb{E} \|D_{u_{j+1}}\| \leq \int_{u_j}^{u_{j+1}} e^{\bar{\mathbf{b}}(s_0)(u_{j+1}-r)} \mathbb{E} \|\delta_r(\tilde{X}_r)\| \, dr.$$

Therefore

$$W_\varphi(p_T P_{0, t_s}, p_{s_0}) \leq \sum_{j=0}^{m-1} \int_{u_j}^{u_{j+1}} e^{-c(t_s - u_{j+1})} e^{\bar{\mathbf{b}}(s_0)(u_{j+1}-r)} \mathbb{E} \|\delta_r(\tilde{X}_r)\| \, dr.$$

Now $\tilde{X}_r \sim p_{T-r}$ for each $r \in [0, t_s]$ by the theorem-level hypothesis, and

$$\mathbb{E} \|\delta_r(\tilde{X}_r)\| = g^2(T-r) \mathbb{E}_{X \sim p_{T-r}} \|e_{T-r}(X)\| \leq g^2(T-r) \varepsilon(T-r)$$

by Cauchy–Schwarz and Assumption 2. Hence the integrand is dominated by

$$e^{(\bar{\mathbf{b}}(s_0)+c)t_s} g^2(T-r) \varepsilon(T-r),$$

which is integrable on $[0, t_s]$. Letting the mesh of the partition tend to zero and using dominated convergence gives

$$W_\varphi(p_T P_{0, t_s}, p_{s_0}) \leq \int_0^{t_s} e^{-c(t_s - r)} \mathbb{E} \|\delta_r(\tilde{X}_r)\| \, dr = \int_{s_0}^T e^{-c(s - s_0)} g^2(s) \mathbb{E}_{X \sim p_s} \|e_s(X)\| \, ds.$$

Applying Cauchy–Schwarz once more yields

$$W_\varphi(p_T P_{0, t_s}, p_{s_0}) \leq \int_{s_0}^T e^{-c(s - s_0)} g^2(s) \varepsilon(s) \, ds. \quad (41)$$

Combine the three pieces. By the triangle inequality,

$$W_\varphi(\text{Law}(Z_{t_s}), p_{s_0}) \leq W_\varphi(\text{Law}(Z_{t_s}), \widehat{p}_T P_{0,t_s}) + W_\varphi(\widehat{p}_T P_{0,t_s}, p_T P_{0,t_s}) + W_\varphi(p_T P_{0,t_s}, p_{s_0}).$$

Substituting (40), the initialization estimate, and (41) proves (39). \square

D Switch-time conversion back to W_2

This section performs the one-time return to Euclidean transport used by our one-switch family. The proof is deliberately specialized to the present switch metric. Because φ_{s_0} has an affine tail, one can decompose D^2 into a small-distance piece controlled by $\varphi_{s_0}(D)$ and a large-distance piece paid for by a p -moment. This produces the exponent θ_p without any additional interpolation machinery and explains why the later sharpness statement is tied to affine-tail costs.

Lemma 15. *Fix an admissible switch $s_0 \in \mathcal{S}_{\text{adm}}$ and $p > 2$. Assume that the switch-time budget $\overline{\mathcal{M}}_p^{\text{sw}}(s_0)$ from (25) is finite. Then*

$$W_2(\text{Law}(Z_{t_s}), p_{s_0}) \leq C_p^{\text{sw}}(s_0) (\Delta_\varphi^{\text{sw}}(s_0))^{\theta_p}, \quad (42)$$

where $C_p^{\text{sw}}(s_0)$ is the switch factor from Section 4.

Proof. The argument is a one-threshold decomposition of D^2 . Small separations are controlled by the linear lower bound $\varphi(r) \geq \alpha r$, while large separations are paid for by the p -moment budget. Let $\varphi := \varphi_{s_0}$, $\alpha := \alpha(s_0)$, and

$$\mu := \text{Law}(Z_{t_s}), \quad \nu := p_{s_0}.$$

By Lemma 11, $\varphi(r) \geq \alpha r$ for all $r \geq 0$.

Fix any coupling (U, V) of (μ, ν) , and set $D := \|U - V\|$. For every $\rho > 0$,

$$D^2 = D^2 \mathbf{1}_{\{D \leq \rho\}} + D^2 \mathbf{1}_{\{D > \rho\}} \leq \rho D + \rho^{-(p-2)} D^p \leq \frac{\rho}{\alpha} \varphi(D) + \rho^{-(p-2)} D^p.$$

Taking expectations and using

$$\mathbb{E}[D^p] \leq 2^{p-1} (\mathbb{E}\|U\|^p + \mathbb{E}\|V\|^p) \leq 2^{p-1} \overline{\mathcal{M}}_p^{\text{sw}}(s_0)$$

gives

$$\mathbb{E}[D^2] \leq \frac{\rho}{\alpha} \mathbb{E}[\varphi(D)] + \frac{2^{p-1} \overline{\mathcal{M}}_p^{\text{sw}}(s_0)}{\rho^{p-2}}.$$

Taking the infimum over couplings yields

$$W_2^2(\mu, \nu) \leq \frac{\rho}{\alpha} W_\varphi(\mu, \nu) + \frac{2^{p-1} \overline{\mathcal{M}}_p^{\text{sw}}(s_0)}{\rho^{p-2}}.$$

Optimizing in ρ gives

$$W_2(\mu, \nu) \leq C_{\text{tr}}(p) \alpha(s_0)^{-\theta_p} (\overline{\mathcal{M}}_p^{\text{sw}}(s_0))^{\frac{1}{2(p-1)}} (W_\varphi(\mu, \nu))^{\theta_p},$$

which is exactly (42). \square

D.1 One explicit admissible moment budget

Proposition 2. *Fix $p > 2$, an admissible switch $s_0 \in \mathcal{S}_{\text{adm}}$, and let $t_s := T - s_0$. Assume the grid contains t_s , say $t_K = t_s$, and suppose*

$$\int_{\mathbb{R}^d} \|y\|^p \Psi_k(x, dy) \leq (1 + A_k) \|x\|^p + B_k, \quad x \in \mathbb{R}^d, \quad k = 0, \dots, K-1,$$

for constants $A_k, B_k \geq 0$. Then

$$\mathbb{E} \|Z_{t_s}\|^p \leq M_{p, \text{num}}^{\text{sw}}(s_0) := \left(\prod_{j=0}^{K-1} (1 + A_j) \right) \mathbb{E}_{Z_0 \sim \widehat{p}_T} \|Z_0\|^p + \sum_{i=0}^{K-1} B_i \prod_{j=i+1}^{K-1} (1 + A_j).$$

Consequently, one admissible choice in (25) is

$$\overline{\mathcal{M}}_p^{\text{sw}}(s_0) = M_{p, \text{num}}^{\text{sw}}(s_0) + \mathbb{E}_{X \sim p_{s_0}} \|X\|^p.$$

Proof. Set $m_k := \mathbb{E} \|Z_{t_k}\|^p$. Since $\text{Law}(Z_{t_{k+1}}) = \text{Law}(Z_{t_k})\Psi_k$, the one-step bound gives

$$m_{k+1} \leq (1 + A_k)m_k + B_k.$$

Iterating this scalar recursion yields the stated bound for $\mathbb{E} \|Z_{t_s}\|^p$. The second claim follows from $\text{Law}(\tilde{X}_{t_s}) = p_{s_0}$ and Lemma 8. \square

D.2 Sharpness of the conversion exponent

The next proposition explains why the exponent $\theta_p = (p-2)/(2(p-1))$ should be viewed as structural rather than incidental. The same affine-tail softness that makes the early metric usable is exactly what limits the price of converting back to W_2 .

Proposition 3. *Fix $p > 2$. Let $\varphi : [0, \infty) \rightarrow [0, \infty)$ be concave, nondecreasing, and affine on $[R_\varphi, \infty)$ with slope $a_\varphi > 0$. Then the exponent*

$$\theta_p := \frac{p-2}{2(p-1)}$$

in the interpolation

$$W_2(\mu, \nu) \lesssim (\mathcal{M}_p(\mu, \nu))^{\frac{1}{2(p-1)}} (W_\varphi(\mu, \nu))^{\theta_p}$$

cannot in general be improved within the class of affine-tail concave costs and p -moment switch assumptions. More precisely, there exist pairs (μ_R, ν_R) with

$$\sup_{R \geq 1} \mathcal{M}_p(\mu_R, \nu_R) < \infty$$

such that

$$W_\varphi(\mu_R, \nu_R) \asymp R^{1-p}, \quad W_2(\mu_R, \nu_R) \asymp R^{1-p/2} \asymp (W_\varphi(\mu_R, \nu_R))^{\theta_p}.$$

Proof. Let $e_1 = (1, 0, \dots, 0)$ and define

$$\mu_R := (1 - R^{-p})\delta_0 + R^{-p}\delta_{Re_1}, \quad \nu_R := \delta_0.$$

Then $\sup_{R \geq 1} \mathcal{M}_p(\mu_R, \nu_R) < \infty$. Since ν_R is a Dirac mass, the unique coupling gives

$$W_2^2(\mu_R, \nu_R) = R^{-p} \|Re_1\|^2 = R^{2-p}, \quad W_\varphi(\mu_R, \nu_R) = R^{-p}\varphi(R).$$

Because φ is affine with positive slope for large R , one has $\varphi(R) \asymp R$, so $W_\varphi(\mu_R, \nu_R) \asymp R^{1-p}$. Hence

$$(W_\varphi(\mu_R, \nu_R))^{\theta_p} \asymp R^{(1-p)\frac{p-2}{2(p-1)}} = R^{1-p/2} = W_2(\mu_R, \nu_R). \quad \square$$

E Late-window Euclidean propagation

After the switch, the radial geometry has already done all of its work. What remains is a purely Euclidean short-horizon propagation problem. Accordingly, this section uses only Euclidean W_2 estimates on $[t_s, T]$ and keeps separate the three quantities that arrive there: the converted switch-time discrepancy, late discretization, and late score forcing.

Proposition 4. *Fix $s_0 \in [0, T]$, let $t_s := T - s_0$, and assume Assumptions 1, 2, and 3. Assume moreover that $\Gamma(s_0) < \infty$, that the learned reverse SDE is strongly well posed on $[t_s, T]$, that the theorem-level ideal reverse SDE (12) admits a global strong solution*

$$(\tilde{X}_t)_{0 \leq t \leq T}$$

with

$$\text{Law}(\tilde{X}_t) = p_{T-t}, \quad 0 \leq t \leq T,$$

that the one-step defects satisfy

$$W_2(P_k(x, \cdot), \Psi_k(x, \cdot)) \leq \xi_k(x), \quad x \in \mathbb{R}^d, \quad k = K, \dots, N-1,$$

and that the relevant second moments are finite. Then

$$W_2(\text{Law}(Z_{t_N}), p_0) \leq \Delta_{\text{late}}^{\text{disc}}(s_0) + e^{\Gamma(s_0)} W_2(\text{Law}(Z_{t_s}), p_{s_0}) + \Delta_{\text{late}}^{\text{force}}(s_0). \quad (43)$$

Proof. Let

$$\mu_k := \text{Law}(Z_{t_k}), \quad \nu_k := \mu_k P_{t_k, T}, \quad k = K, \dots, N.$$

Then

$$\nu_N = \text{Law}(Z_{t_N}), \quad \nu_K = \mu_K P_{t_s, T}.$$

late discretization. By the triangle inequality,

$$W_2(\nu_N, \nu_K) \leq \sum_{k=K}^{N-1} W_2(\nu_{k+1}, \nu_k).$$

Since

$$\nu_{k+1} = (\mu_k \Psi_k) P_{t_{k+1}, T}, \quad \nu_k = (\mu_k P_k) P_{t_{k+1}, T},$$

it remains to propagate one-step defects from t_{k+1} to T .

Fix $k \in \{K, \dots, N-1\}$, and let $\alpha, \beta \in \mathcal{P}_2(\mathbb{R}^d)$. Choose any coupling $\pi \in \Pi(\alpha, \beta)$, let $(Y_{t_{k+1}}, \bar{Y}_{t_{k+1}}) \sim \pi$, and let Y, \bar{Y} solve the learned reverse SDE on $[t_{k+1}, T]$ driven by the same Brownian motion. Set

$$D_t := Y_t - \bar{Y}_t.$$

Because the noise is synchronized, D is absolutely continuous and

$$\dot{D}_t = \widehat{b}_t(Y_t) - \widehat{b}_t(\bar{Y}_t) \quad \text{for a.e. } t \in [t_{k+1}, T].$$

By Lemma 1(iii),

$$\langle D_t, \widehat{b}_t(Y_t) - \widehat{b}_t(\bar{Y}_t) \rangle \leq \mathfrak{b}(T-t) \|D_t\|^2 \quad \text{for a.e. } t \in [t_{k+1}, T].$$

Applying Lemma 12 with

$$A_t := \widehat{b}_t(Y_t) - \widehat{b}_t(\bar{Y}_t), \quad F_t := 0, \quad \beta(t) := \mathfrak{b}(T-t),$$

yields

$$\|D_T\| \leq e^{\int_{t_{k+1}}^T \mathfrak{b}(T-r) \, dr} \|D_{t_{k+1}}\| = e^{\Gamma(T-t_{k+1})} \|D_{t_{k+1}}\|.$$

Squaring and taking expectations gives

$$\mathbb{E} \|D_T\|^2 \leq e^{2\Gamma(T-t_{k+1})} \mathbb{E} \|D_{t_{k+1}}\|^2.$$

Since π was arbitrary, taking the infimum over all $\pi \in \Pi(\alpha, \beta)$ yields

$$W_2(\alpha P_{t_{k+1}, T}, \beta P_{t_{k+1}, T}) \leq e^{\Gamma(T-t_{k+1})} W_2(\alpha, \beta).$$

Applying this with $\alpha = \mu_k \Psi_k$ and $\beta = \mu_k P_k$ gives

$$W_2(\nu_{k+1}, \nu_k) \leq e^{\Gamma(T-t_{k+1})} W_2(\mu_k \Psi_k, \mu_k P_k).$$

Apply Zhang [2013, Theorem 1.1] on the parameter space $(\mathbb{R}^d, \mathcal{B}(\mathbb{R}^d), \mu_k)$ with

$$\mu_x := \Psi_k(x, \cdot), \quad \nu_x := P_k(x, \cdot), \quad c(y, z) := \|y - z\|^2.$$

This yields a Borel measurable family

$$x \mapsto \pi_k^x \in \Pi(\Psi_k(x, \cdot), P_k(x, \cdot))$$

of optimal couplings for the quadratic cost. Integrating π_k^x against $\mu_k(dx)$ gives a coupling of $\mu_k \Psi_k$ and $\mu_k P_k$, and therefore

$$W_2^2(\mu_k \Psi_k, \mu_k P_k) \leq \int_{\mathbb{R}^d} W_2^2(\Psi_k(x, \cdot), P_k(x, \cdot)) \mu_k(dx) \leq \mathbb{E}[\xi_k(Z_{t_k})^2].$$

Therefore

$$W_2(\nu_{k+1}, \nu_k) \leq e^{\Gamma(T-t_{k+1})} \left(\mathbb{E}[\xi_k(Z_{t_k})^2] \right)^{1/2}.$$

Summing over $k = K, \dots, N-1$ yields

$$W_2(\text{Law}(Z_{t_N}), \mu_K P_{t_s, T}) \leq \Delta_{\text{late}}^{\text{disc}}(s_0). \quad (44)$$

switch-time discrepancy and late score forcing. We separate the switch-time mismatch from the forcing accumulated after the switch:

$$W_2(\mu_K P_{t_s, T}, p_0) \leq W_2(\mu_K P_{t_s, T}, p_{s_0} P_{t_s, T}) + W_2(p_{s_0} P_{t_s, T}, p_0).$$

For the first term, choose an optimal coupling $\pi \in \Pi(\mu_K, p_{s_0})$, let $(Y_{t_s}, \bar{Y}_{t_s}) \sim \pi$, and let Y, \bar{Y} solve the learned reverse SDE on $[t_s, T]$ driven by the same Brownian motion. Set

$$D_t := Y_t - \bar{Y}_t.$$

Because the noise is synchronized,

$$\dot{D}_t = \widehat{b}_t(Y_t) - \widehat{b}_t(\bar{Y}_t) \quad \text{for a.e. } t \in [t_s, T].$$

By Lemma 1(iii),

$$\langle D_t, \widehat{b}_t(Y_t) - \widehat{b}_t(\bar{Y}_t) \rangle \leq \mathfrak{b}(T-t) \|D_t\|^2 \quad \text{for a.e. } t \in [t_s, T].$$

Applying Lemma 12 with $F_t := 0$ and $\beta(t) := \mathfrak{b}(T-t)$ yields

$$\|D_T\| \leq e^{\int_{t_s}^T \mathfrak{b}(T-r) \, dr} \|D_{t_s}\| = e^{\Gamma(s_0)} \|D_{t_s}\|.$$

Squaring, taking expectations, and using the optimality of π give

$$W_2(\mu_K P_{t_s, T}, p_{s_0} P_{t_s, T}) \leq e^{\Gamma(s_0)} W_2(\mu_K, p_{s_0}) = e^{\Gamma(s_0)} W_2(\text{Law}(Z_{t_s}), p_{s_0}).$$

It remains to control $W_2(p_{s_0} P_{t_s, T}, p_0)$. Let \tilde{X} be the global ideal reverse solution from the theorem-level hypothesis. Because the learned reverse SDE is strongly well posed on $[t_s, T]$, on the same filtered space and with the same Brownian motion \tilde{B} that drives \tilde{X} , there exists a unique strong solution Y^* of the learned reverse SDE on $[t_s, T]$ with

$$Y_{t_s}^* = \tilde{X}_{t_s}.$$

Since $\text{Law}(\tilde{X}_{t_s}) = p_{s_0}$, the Markov property gives

$$\text{Law}(Y_T^*) = p_{s_0} P_{t_s, T}.$$

Moreover,

$$\text{Law}(\tilde{X}_r) = p_{T-r} \quad \text{for all } r \in [t_s, T], \quad \text{in particular} \quad \text{Law}(\tilde{X}_T) = p_0.$$

Set

$$D_t := Y_t^* - \tilde{X}_t.$$

Because the Brownian motions are identical,

$$\dot{D}_t = \widehat{b}_t(Y_t^*) - \widehat{b}_t(\tilde{X}_t) + \delta_t(\tilde{X}_t) \quad \text{for a.e. } t \in [t_s, T].$$

By Lemma 1(iii),

$$\langle D_t, \widehat{b}_t(Y_t^*) - \widehat{b}_t(\tilde{X}_t) \rangle \leq \mathfrak{b}(T-t) \|D_t\|^2 \quad \text{for a.e. } t \in [t_s, T].$$

Applying Lemma 12 with

$$A_t := \widehat{b}_t(Y_t^*) - \widehat{b}_t(\tilde{X}_t), \quad F_t := \delta_t(\tilde{X}_t), \quad \beta(t) := \mathfrak{b}(T-t),$$

and using $D_{t_s} = 0$ gives

$$\|D_T\| \leq \int_{t_s}^T e^{\int_r^T \mathfrak{b}(T-\tau) \, d\tau} \|\delta_r(\tilde{X}_r)\| \, dr = \int_{t_s}^T e^{\Gamma(T-r)} \|\delta_r(\tilde{X}_r)\| \, dr.$$

Taking the L^2 -norm and using Minkowski's integral inequality yields

$$(\mathbb{E} \|D_T\|^2)^{1/2} \leq \int_{t_s}^T e^{\Gamma(T-r)} (\mathbb{E} \|\delta_r(\tilde{X}_r)\|^2)^{1/2} \, dr.$$

Also, since $\tilde{X}_r \sim p_{T-r}$,

$$(\mathbb{E} \|\delta_r(\tilde{X}_r)\|^2)^{1/2} = g^2(T-r) \left(\mathbb{E}_{X \sim p_{T-r}} \|e_{T-r}(X)\|^2 \right)^{1/2} \leq g^2(T-r) \varepsilon(T-r)$$

by Assumption 2. Therefore the coupling (Y_T^*, \tilde{X}_T) gives

$$W_2(p_{s_0} P_{t_s, T}, p_0) \leq (\mathbb{E} \|D_T\|^2)^{1/2} \leq \int_{t_s}^T e^{\Gamma(T-r)} g^2(T-r) \varepsilon(T-r) \, dr.$$

Changing variables $s = T - r$ gives

$$W_2(p_{s_0} P_{t_s, T}, p_0) \leq \Delta_{\text{late}}^{\text{force}}(s_0). \quad (45)$$

Combining the two bounds proves

$$W_2(\mu_K P_{t_s, T}, p_0) \leq e^{\Gamma(s_0)} W_2(\text{Law}(Z_{t_s}), p_{s_0}) + \Delta_{\text{late}}^{\text{force}}(s_0). \quad (46)$$

combine the two late pieces. Combining (44) with (46) and the triangle inequality proves (43). \square

F Main theorem proof and Euclidean comparison

F.1 Proof of the main theorem and switch selection

Proof of Theorem 1. Fix an admissible grid-aligned switch $s_0 \in \mathcal{S}_{\text{adm}}$, with $t_K = t_s := T - s_0$. By Lemma 14,

$$\Delta_{\varphi}^{\text{sw}}(s_0) \leq \overline{\Delta}_{\varphi}^{\text{sw}}(s_0).$$

By Lemma 15,

$$W_2(\text{Law}(Z_{t_s}), p_{s_0}) \leq C_p^{\text{sw}}(s_0) (\Delta_{\varphi}^{\text{sw}}(s_0))^{\theta_p} \leq C_p^{\text{sw}}(s_0) (\overline{\Delta}_{\varphi}^{\text{sw}}(s_0))^{\theta_p}.$$

Finally, Proposition 4 yields

$$W_2(\text{Law}(Z_{t_N}), p_0) \leq \Delta_{\text{late}}(s_0) + e^{\Gamma(s_0)} W_2(\text{Law}(Z_{t_s}), p_{s_0}).$$

Substituting the switch-time conversion estimate proves (26). \square

Definition 7 (Scalar switch-selection objective). For an admissible grid-aligned switch $s_0 \in \mathcal{S}_{\text{adm}}$, define

$$\mathcal{B}_p(s_0) := \Delta_{\text{late}}(s_0) + e^{\Gamma(s_0)} C_p^{\text{sw}}(s_0) \left(\overline{\Delta}_{\varphi}^{\text{sw}}(s_0) \right)^{\theta_p}. \quad (47)$$

Corollary 2 (Discrete one-switch selection principle). *Define the admissible grid*

$$\mathcal{S}_{\text{adm}}^h := \mathcal{S}_{\text{adm}} \cap \{T - t_k : k = 1, \dots, N - 1\}.$$

Under the assumptions of Theorem 1, every switch $s_0 \in \mathcal{S}_{\text{adm}}^h$ satisfies

$$W_2(\text{Law}(Z_{t_N}), p_0) \leq \mathcal{B}_p(s_0).$$

Consequently, whenever $\mathcal{S}_{\text{adm}}^h \neq \emptyset$, there exists $s_0^ \in \mathcal{S}_{\text{adm}}^h$ such that*

$$\mathcal{B}_p(s_0^*) = \min_{s_0 \in \mathcal{S}_{\text{adm}}^h} \mathcal{B}_p(s_0), \quad W_2(\text{Law}(Z_{t_N}), p_0) \leq \mathcal{B}_p(s_0^*).$$

Remark 8 (Why one-switch selection is nontrivial). Admissibility and optimization play different roles. Admissibility is a geometric existence statement: it says that on the whole early window the far field carries a positive contraction reserve. Optimization is a geometric routing statement *within the one-switch family* studied in this paper: it decides when one should stop using the soft radial metric, pay the one-time conversion back to W_2 , and expose the remaining error to the late Euclidean load. We do not claim here that this scalar optimization is globally optimal among multi-switch or continuously varying metric strategies.

Proof of Corollary 2. The first claim is immediate from Theorem 1 and Definition 7. Since $\mathcal{S}_{\text{adm}}^h$ is finite whenever nonempty, \mathcal{B}_p attains a minimum on $\mathcal{S}_{\text{adm}}^h$, and applying Theorem 1 at a minimizer gives the second claim. \square

F.2 Formal comparison with the direct full-horizon Euclidean route

Proposition 5 (Direct full-horizon Euclidean propagation). *Assume Assumptions 1, 2, and 3, that $\Gamma(T) < \infty$, and that the learned reverse SDE is strongly well posed on $[0, T]$. Assume moreover that the one-step numerical defects satisfy*

$$W_2(P_k(x, \cdot), \Psi_k(x, \cdot)) \leq \xi_k(x), \quad x \in \mathbb{R}^d, \quad k = 0, \dots, N - 1,$$

and that the relevant second moments are finite. Then

$$\begin{aligned} W_2(\text{Law}(Z_{t_N}), p_0) &\leq e^{\Gamma(T)} W_2(\widehat{p}_T, p_T) + \sum_{k=0}^{N-1} e^{\Gamma(T-t_{k+1})} \left(\mathbb{E}[\xi_k(Z_{t_k})^2] \right)^{1/2} \\ &\quad + \int_0^T e^{\Gamma(s)} g^2(s) \varepsilon(s) \, ds. \end{aligned} \quad (48)$$

Proof. Apply Proposition 4 with the candidate switch $s_0 = T$. Then $t_s = 0$, $K = 0$, and $p_{s_0} = p_T$. The late-window bound becomes exactly (48). \square

Corollary 3 (Formal comparison with the direct full-horizon Euclidean route). *Assume the hypotheses of Theorem 1 and of Proposition 5. Fix an admissible grid-aligned switch $s_0 \in \mathcal{S}_{\text{adm}}$, with $t_K = t_s := T - s_0$. Define*

$$\begin{aligned} \mathcal{D}_{\text{dir}}(s_0) &:= \Delta_{\text{late}}^{\text{disc}}(s_0) + \Delta_{\text{late}}^{\text{force}}(s_0) \\ &+ e^{\Gamma(T)} W_2(\widehat{p}_T, p_T) + \sum_{k=0}^{K-1} e^{\Gamma(T-t_{k+1})} \left(\mathbb{E}[\xi_k(Z_{t_k})^2] \right)^{1/2} + \int_{s_0}^T e^{\Gamma(s)} g^2(s) \varepsilon(s) \, ds. \end{aligned} \quad (49)$$

Then

$$W_2(\text{Law}(Z_{t_N}), p_0) \leq \min\{\mathcal{B}_p(s_0), \mathcal{D}_{\text{dir}}(s_0)\}.$$

Proof. The phase-aware part is exactly Theorem 1 packaged by Definition 7. The direct part comes from Proposition 5 by splitting the sum and the integral at the grid index K . \square

Remark 9 (What the comparison isolates). The direct Euclidean route and the phase-aware route differ only in how they transport the pre-switch terms. The direct route sends initialization mismatch, pre-switch discretization, and pre-switch score forcing directly through the full-horizon Euclidean weights. By contrast, the phase-aware route first compresses the same three inputs inside $\overline{\Delta}_{\varphi}^{\text{sw}}(s_0)$, pays the one-time conversion back to W_2 , and only then incurs the shorter late-window factor $e^{\Gamma(s_0)}$. Thus the gain is structural: it comes from routing the same early errors through different geometries.

G Operational supplements: proxy switches and verification

Nothing in this section is needed for the proof of Theorem 1. Its role is operational: to compare Assumption 3 with more classical global score-regularity hypotheses, to record conservative proxy switches, to give verifiable sufficient conditions for the early reflection-coupling input, and to exhibit a concrete worked example in which the one-switch theorem can be instantiated explicitly.

G.1 Assumption 3 compared with global score regularity

Remark 10 (Structural versus verification assumptions). Assumption 3 is the structural geometric hypothesis used by the theorem. It enters only through the one-sided loss $\ell(s)$, which perturbs the radial profile and the late Euclidean load. By contrast, global Lipschitz assumptions on the score error e_s , or on the learned score $s_{\theta}(\cdot, s)$ together with the true score $\nabla \log p_s$, are stronger verification devices. They are useful because they imply Assumption 3 and also fit naturally with the well-posedness and reflection-coupling input used later, but they are not the quantities that the geometric argument itself sees.

Lemma 16 (Jacobian and Lipschitz criteria for Assumption 3). *Suppose that for a.e. $s \in (0, T]$, one of the following holds:*

- (a) *the map $x \mapsto e_s(x)$ is C^1 , and there exists a measurable $\bar{\ell} : (0, T] \rightarrow \mathbb{R}$ such that*

$$\lambda_{\max} \left(\frac{1}{2} (\nabla e_s(x) + \nabla e_s(x)^{\top}) \right) \leq \bar{\ell}(s), \quad x \in \mathbb{R}^d;$$

- (b) *there exists a measurable $L_e : (0, T] \rightarrow [0, \infty)$ such that*

$$\|e_s(x) - e_s(y)\| \leq L_e(s) \|x - y\|, \quad x, y \in \mathbb{R}^d;$$

- (c) *there exist measurable $L_{\theta}, L_{\star} : (0, T] \rightarrow [0, \infty)$ such that for $x, y \in \mathbb{R}^d$*

$$\|s_{\theta}(x, s) - s_{\theta}(y, s)\| \leq L_{\theta}(s) \|x - y\|, \quad \|\nabla \log p_s(x) - \nabla \log p_s(y)\| \leq L_{\star}(s) \|x - y\|.$$

Then Assumption 3 holds with

$$\ell(s) = \bar{\ell}(s) \quad \text{in case (a),} \quad \ell(s) = L_e(s) \quad \text{in case (b),} \quad \ell(s) = L_{\theta}(s) + L_{\star}(s) \quad \text{in case (c).}$$

Proof. Case (a) is the standard symmetrized-Jacobian criterion. Fix s such that the assumption holds and let $x, y \in \mathbb{R}^d$. Writing $\gamma(\tau) = y + \tau(x - y)$, one has

$$e_s(x) - e_s(y) = \int_0^1 \nabla e_s(\gamma(\tau))(x - y) \, d\tau.$$

Taking the inner product with $x - y$, symmetrizing, and using the eigenvalue bound gives

$$\langle e_s(x) - e_s(y), x - y \rangle \leq \bar{\ell}(s) \|x - y\|^2.$$

For case (b), Cauchy–Schwarz gives

$$\langle e_s(x) - e_s(y), x - y \rangle \leq \|e_s(x) - e_s(y)\| \|x - y\| \leq L_e(s) \|x - y\|^2.$$

For case (c), since

$$e_s(x) - e_s(y) = (s_\theta(x, s) - s_\theta(y, s)) - (\nabla \log p_s(x) - \nabla \log p_s(y)),$$

the triangle inequality yields

$$\|e_s(x) - e_s(y)\| \leq (L_\theta(s) + L_*(s)) \|x - y\|,$$

and case (b) applies. \square

G.2 A computable proxy for admissibility and switch selection

Proposition 6 (Conservative proxy switches and proxy objective). *Assume Assumptions 1, 2 and 3, and suppose that $\ell(s) \leq \bar{\ell}(s)$ and $\varepsilon(s) \leq \bar{\varepsilon}(s)$ for a.e. $s \in (0, T]$, where $\bar{\ell} : (0, T] \rightarrow \mathbb{R}$ and $\bar{\varepsilon} : (0, T] \rightarrow [0, \infty)$ are measurable. Define*

$$\mathbf{m}_{\text{pr}}(s) := g^2(s)(\alpha_s - \bar{\ell}(s)) - f(s), \quad \mathbf{b}_{\text{pr}}(s) := f(s) + g^2(s)(M_s + \bar{\ell}(s) - \alpha_s).$$

Then every grid-aligned s_0 with

$$\underline{m}_{\text{pr}}(s_0) := \inf_{u \in [s_0, T]} \mathbf{m}_{\text{pr}}(u) > 0$$

is admissible, and the proof of Theorem 1 goes through with the conservative replacements

$$\mathbf{m}, \mathbf{b}, \varepsilon \rightsquigarrow \mathbf{m}_{\text{pr}}, \mathbf{b}_{\text{pr}}, \bar{\varepsilon}.$$

In particular, every such switch yields a certified proxy bound

$$W_2(\text{Law}(Z_{t_N}), p_0) \leq \mathcal{B}_p^{\text{pr}}(s_0),$$

where $\mathcal{B}_p^{\text{pr}}(s_0)$ is obtained from $\mathcal{B}_p(s_0)$ by replacing the exact geometric inputs by their proxy versions.

Proof. Introduce the proxy lower envelope

$$\underline{\kappa}_s^{\text{pr}}(r) := g^2(s) \left(\alpha_s - \frac{1}{r} f_{M_s}(r) - \bar{\ell}(s) \right) - f(s).$$

Since $\ell(s) \leq \bar{\ell}(s)$, one has

$$\underline{\kappa}_s(r) \geq \underline{\kappa}_s^{\text{pr}}(r), \quad r > 0, \, s \in (0, T].$$

Taking $r \downarrow 0$ and $r \rightarrow \infty$ shows

$$\mathbf{m}(s) \geq \mathbf{m}_{\text{pr}}(s), \quad \mathbf{b}(s) \leq \mathbf{b}_{\text{pr}}(s), \quad s \in (0, T].$$

Hence $\underline{m}_{\text{pr}}(s_0) > 0$ implies $\underline{m}(s_0) > 0$, so every proxy-admissible switch is genuinely admissible.

The remaining claim follows by monotonicity of the constructions used in the proof: a smaller lower profile can only worsen the early contraction input, a larger forcing bound $\bar{\varepsilon}$ can only enlarge the forcing terms, and a larger Euclidean load \mathbf{b}_{pr} can only enlarge the late propagation factor. Rerunning the early contraction, switch conversion, and late Euclidean propagation arguments with $\underline{\kappa}^{\text{pr}}, \mathbf{m}_{\text{pr}}, \mathbf{b}_{\text{pr}}, \bar{\varepsilon}$ therefore produces a certified upper bound $\mathcal{B}_p^{\text{pr}}(s_0)$. \square

G.3 Verifiable sufficient conditions for the early reflection-coupling input

Proposition 7 (A convenient sufficient condition for the early coupling input). *Fix an admissible switch $s_0 \in \mathcal{S}_{\text{adm}}$ and write $t_s := T - s_0$. Assume:*

- (a) g is continuous on $[s_0, T]$ and $\underline{g}(s_0) > 0$;
- (b) the map $(t, x) \mapsto \widehat{b}_t(x)$ is Borel measurable on $[0, t_s] \times \mathbb{R}^d$;
- (c) there exists $L_{s_0} < \infty$ such that

$$\|\widehat{b}_t(x) - \widehat{b}_t(y)\| \leq L_{s_0} \|x - y\|, \quad t \in [0, t_s], \quad x, y \in \mathbb{R}^d;$$

- (d) there exists $B_{s_0} < \infty$ such that

$$\|\widehat{b}_t(x)\| \leq B_{s_0}(1 + \|x\|), \quad t \in [0, t_s], \quad x \in \mathbb{R}^d.$$

Then the learned reverse SDE (13) is strongly well posed on $[0, t_s]$. Moreover, for every initial coupling $\pi \in \Pi(\mu, \nu)$ with $\mu, \nu \in \mathcal{P}_1(\mathbb{R}^d)$ and every subinterval $[u, v] \subseteq [0, t_s]$, there exists a coalescing reflection coupling in the sense of Definition 5; see Eberle [2016], Eberle et al. [2019].

Proof. Assumptions (b)–(d) are the standard measurable, global-Lipschitz, and linear-growth hypotheses yielding strong existence and pathwise uniqueness for (13) on $[0, t_s]$.

Fix a subinterval $[u, v] \subseteq [0, t_s]$ and an initial coupling $\pi \in \Pi(\mu, \nu)$. Because the diffusion coefficient is the deterministic isotropic matrix

$$g(T - t)I_d,$$

with g continuous and bounded away from 0 on $[u, v]$ by (a), the standard reflection-coupling construction for isotropic diffusions with globally Lipschitz drift applies on $[u, v]$: one reflects the driving Brownian motion across the hyperplane orthogonal to the current separation vector up to the meeting time and switches to synchronous coupling afterwards. See Eberle [2016, Section 2] and Eberle et al. [2019, Section 2.1]. The present coefficient differs from the unit-diffusion case only by a deterministic scalar factor, so the same construction extends directly on each finite subinterval. Therefore, for every initial coupling π , there exists a coalescing reflection coupling in the sense of Definition 5. \square

Corollary 4 (A network-level checklist). *Fix an admissible switch $s_0 \in \mathcal{S}_{\text{adm}}$. Assume g is continuous on $[s_0, T]$ with $\underline{g}(s_0) > 0$, that f and g are bounded on $[s_0, T]$, and that there exist constants $L_\theta(s_0), B_{\theta,0}(s_0) < \infty$ such that*

$$\|s_\theta(x, s) - s_\theta(y, s)\| \leq L_\theta(s_0) \|x - y\|, \quad \|s_\theta(0, s)\| \leq B_{\theta,0}(s_0), \quad s \in [s_0, T], \quad x, y \in \mathbb{R}^d.$$

Then Proposition 7 applies. In particular, the coupling input required by Lemma 13 is automatic.

Proof. For $t \in [0, t_s]$,

$$\widehat{b}_t(x) - \widehat{b}_t(y) = f(T - t)(x - y) + g^2(T - t)(s_\theta(x, T - t) - s_\theta(y, T - t)),$$

hence

$$\|\widehat{b}_t(x) - \widehat{b}_t(y)\| \leq \left(\|f\|_{L^\infty([s_0, T])} + \|g\|_{L^\infty([s_0, T])}^2 L_\theta(s_0) \right) \|x - y\|.$$

Likewise,

$$\|\widehat{b}_t(x)\| \leq \|f\|_{L^\infty([s_0, T])} \|x\| + \|g\|_{L^\infty([s_0, T])}^2 \left(\|s_\theta(0, T - t)\| + L_\theta(s_0) \|x\| \right),$$

so

$$\|\widehat{b}_t(x)\| \leq B_{s_0}(1 + \|x\|)$$

for a suitable finite B_{s_0} . Thus all hypotheses of Proposition 7 are satisfied. \square

G.4 Worked example: a variance-preserving schedule with Euler/Heun-type defects

Proposition 8 (Explicit proxy geometry and a concrete admissible regime in the VP example).
Consider the variance-preserving schedule

$$f(s) \equiv \frac{\beta}{2}, \quad g(s) \equiv \sqrt{\beta}, \quad \beta > 0,$$

and assume the proxy bounds

$$\ell(s) \leq \bar{\ell}, \quad \varepsilon(s) \leq \bar{\varepsilon}, \quad s \in (0, T],$$

for constants $\bar{\ell} \in \mathbb{R}$ and $\bar{\varepsilon} \geq 0$. Define

$$D(s) := \alpha + (1 - \alpha)e^{-\beta s}.$$

Then

$$a(s) = e^{-\beta s/2}, \quad \sigma^2(s) = 1 - e^{-\beta s}, \quad \alpha_s = \frac{\alpha}{D(s)}, \quad M_s = \frac{M e^{-\beta s}}{D(s)^2}.$$

Consequently the proxy reserve and load are

$$\mathbf{m}_{\text{pr}}(s) = \beta \left(\frac{\alpha}{D(s)} - \bar{\ell} - \frac{1}{2} \right), \quad \mathbf{b}_{\text{pr}}(s) = \beta \left(\frac{M e^{-\beta s}}{D(s)^2} + \bar{\ell} + \frac{1}{2} - \frac{\alpha}{D(s)} \right).$$

If $\alpha < 1$ and $\bar{\ell} < \frac{1}{2}$, define

$$s_{\text{pr}}^* := \max \left\{ 0, \frac{1}{\beta} \log \left(\frac{(\bar{\ell} + \frac{1}{2})(1 - \alpha)}{\alpha(\frac{1}{2} - \bar{\ell})} \right) \right\}.$$

Then every grid-aligned $s_0 \in [s_{\text{pr}}^*, T]$ is proxy-admissible, provided $s_{\text{pr}}^* \leq T$.

Moreover, the proxy late-window load is explicit:

$$\Gamma_{\text{pr}}(s_0) := \int_0^{s_0} \mathbf{b}_{\text{pr}}(u) \, du = \beta \left(\bar{\ell} + \frac{1}{2} \right) s_0 - \log(\alpha e^{\beta s_0} + 1 - \alpha) + \mathcal{M}_{\text{VP}}(s_0),$$

where

$$\mathcal{M}_{\text{VP}}(s_0) := \begin{cases} \frac{M}{1 - \alpha} \left(\frac{1}{D(s_0)} - 1 \right), & \alpha \neq 1, \\ M(1 - e^{-\beta s_0}), & \alpha = 1. \end{cases}$$

If, in addition, the numerical grid is uniform, $t_k = kh$, and

$$\left(\mathbb{E}[\xi_k(Z_{t_k})^2] \right)^{1/2} \leq C_{\text{sch}} h^q, \quad k = 0, \dots, N - 1,$$

then every proxy-admissible grid-aligned switch s_0 yields a concrete one-switch bound

$$W_2(\text{Law}(Z_{t_N}), p_0) \leq \Delta_{\text{late}}^{\text{pr}}(s_0) + e^{\Gamma_{\text{pr}}(s_0)} C_{p, \text{pr}}^{\text{sw}}(s_0) \left(\overline{\Delta}_{\varphi, \text{pr}}^{\text{sw}}(s_0) \right)^{\theta_p},$$

with

$$\overline{\Delta}_{\varphi, \text{pr}}^{\text{sw}}(s_0) \lesssim e^{-c_{\text{pr}}(s_0)(T-s_0)} W_{\varphi_{s_0}^{\text{pr}}}(\widehat{p}_T, p_T) + C_{\text{sch}}(T - s_0) h^{q-1} + \frac{\beta \bar{\varepsilon}}{c_{\text{pr}}(s_0)} \left(1 - e^{-c_{\text{pr}}(s_0)(T-s_0)} \right),$$

and

$$\Delta_{\text{late}}^{\text{pr}}(s_0) \lesssim C_{\text{sch}} s_0 h^{q-1} \sup_{u \in [0, s_0]} e^{\Gamma_{\text{pr}}(u)} + \beta \bar{\varepsilon} \int_0^{s_0} e^{\Gamma_{\text{pr}}(u)} \, du.$$

By contrast, the direct full-horizon Euclidean route gives only

$$W_2(\text{Law}(Z_{t_N}), p_0) \lesssim e^{\Gamma_{\text{pr}}(T)} W_2(\widehat{p}_T, p_T) + C_{\text{sch}} T h^{q-1} \sup_{u \in [0, T]} e^{\Gamma_{\text{pr}}(u)} + \beta \bar{\varepsilon} \int_0^T e^{\Gamma_{\text{pr}}(u)} \, du.$$

Proof. Under the VP schedule,

$$a(s) = \exp\left(-\int_0^s \frac{\beta}{2} du\right) = e^{-\beta s/2},$$

and

$$\sigma^2(s) = \int_0^s e^{-\beta(s-u)} \beta du = 1 - e^{-\beta s}.$$

Substituting these into (16) gives

$$\alpha_s = \frac{\alpha}{\alpha + (1-\alpha)e^{-\beta s}} = \frac{\alpha}{D(s)}, \quad M_s = \frac{M e^{-\beta s}}{D(s)^2}.$$

The formulas for m_{pr} and b_{pr} follow immediately from Definition 3 with ℓ replaced by $\bar{\ell}$.

Assume now $\alpha < 1$. Then $s \mapsto \alpha_s$ is increasing, so

$$m_{\text{pr}}(s_0) > 0 \iff m_{\text{pr}}(s_0) > 0 \iff \frac{\alpha}{D(s_0)} > \bar{\ell} + \frac{1}{2}.$$

Solving this inequality gives exactly $s_0 \geq s_{\text{pr}}^*$.

For the load, write

$$\Gamma_{\text{pr}}(s_0) = \beta \left(\bar{\ell} + \frac{1}{2}\right) s_0 + \beta \int_0^{s_0} \frac{M e^{-\beta u}}{D(u)^2} du - \beta \int_0^{s_0} \frac{\alpha}{D(u)} du.$$

The last two integrals are explicit:

$$\beta \int_0^{s_0} \frac{\alpha}{D(u)} du = \log(\alpha e^{\beta s_0} + 1 - \alpha),$$

and

$$\beta \int_0^{s_0} \frac{M e^{-\beta u}}{D(u)^2} du = \mathcal{M}_{\text{VP}}(s_0),$$

with the stated formula for $\alpha \neq 1$, and the $\alpha = 1$ case obtained by direct integration.

For the discretization terms, the uniform one-step bound gives

$$\sum_{k=0}^{K-1} e^{-c_{\text{pr}}(s_0)(t_s - t_{k+1})} \left(\mathbb{E}[\xi_k(Z_{t_k})^2]\right)^{1/2} \leq C_{\text{sch}} h^q \sum_{k=0}^{K-1} 1 \leq C_{\text{sch}} (T - s_0) h^{q-1},$$

and similarly

$$\sum_{k=K}^{N-1} e^{\Gamma_{\text{pr}}(T - t_{k+1})} \left(\mathbb{E}[\xi_k(Z_{t_k})^2]\right)^{1/2} \leq C_{\text{sch}} s_0 h^{q-1} \sup_{u \in [0, s_0]} e^{\Gamma_{\text{pr}}(u)}.$$

Because $\bar{\varepsilon}$ is constant, the early forcing term is

$$\int_{s_0}^T e^{-c_{\text{pr}}(s_0)(s-s_0)} \beta \bar{\varepsilon} ds = \frac{\beta \bar{\varepsilon}}{c_{\text{pr}}(s_0)} \left(1 - e^{-c_{\text{pr}}(s_0)(T-s_0)}\right).$$

The stated one-switch bound then follows from Proposition 6 and Theorem 1, applied with the proxy inputs. The direct Euclidean comparison is the corresponding specialization of the full-horizon Euclidean bound. \square